



THESIS

2



This is to certify that the
thesis entitled

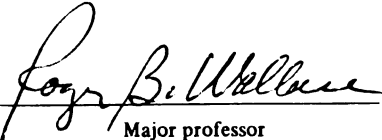
HYDRAULIC CONDUCTIVITY OF SORPTIVE ZONES CREATED BY
IN_SITU INJECTION OF A CATIONIC SURFACTANT

presented by

William James Gellner II

has been accepted towards fulfillment
of the requirements for

M.S. degree in Environmental
Engineering


Major professor

Date January 2, 1997

PLACE IN RETURN BOX to remove this checkout from your record.
TO AVOID FINES return on or before date due.

DATE DUE	DATE DUE	DATE DUE
_____	_____	_____
_____	_____	_____
_____	_____	_____
_____	_____	_____
_____	_____	_____
_____	_____	_____
_____	_____	_____

MSU is An Affirmative Action/Equal Opportunity Institution

c:\circ\datedue.pm3-p.1

**HYDRAULIC CONDUCTIVITY OF SORPTIVE ZONES CREATED BY IN-SITU
INJECTION OF A CATIONIC SURFACTANT**

By

William James Gellner II

A THESIS

**Submitted to
Michigan State University
in partial fulfillment of the requirements
for the degree of**

MASTER OF SCIENCE

Department of Civil and Environmental Engineering

1997

ABSTRACT

HYDRAULIC CONDUCTIVITY OF SORPTIVE ZONES CREATED BY IN-SITU INJECTION OF A CATIONIC SURFACTANT

By

William James Gellner II

The hydraulic properties of sorptive zones created by *in-situ* injection of the cationic surfactant hexadecyltrimethylammonium (HDTMA) was investigated. Oshtemo B soil (87% sand, 10.5% clay, 2.5% silt) subjected to two different effective stresses was treated by recirculation to two different HDTMA soil concentrations. Results indicate that no drastic changes in hydraulic conductivity occurred. Therefore, sorptive zones created *in-situ* with HDTMA appear hydraulically feasible in soils with dispersed clays. Changes in hydraulic conductivity were attributable to changes in effective pore size, likely caused by clay migration and pore blocking. The degree of conductivity change was related to the degree of clay dispersion induced by treatment. Those treatment conditions which resulted in more clay dispersion, indicated by higher turbidity, caused greater decreases in conductivity. Therefore, turbidity measurements may serve as a qualitative indicator of changes in hydraulic conductivity that can be expected due to treatment.

This thesis and all of the work it represents is dedicated to my fiancé, Lili, and my family.

Lili has shown me love and support I have never experienced before and she has made me whole. My parents have each, in their own way, loved and supported me throughout my life and have shaped me into the person that I have become. My brothers, Bob and Matt, have given me the joy that only siblings can give. Without any one of these people I would not be where I am now.

ACKNOWLEDGMENTS

This research was supported by the National Institute for Environmental Health Sciences grant #ES04911 and the Michigan State University Institute for Environmental Toxicology. I would like to thank my advisor, Dr. Roger B. Wallace, for his support of this work. I am very grateful for the opportunity to work under his guidance and I will forever be indebted to him for his academic and personal advice throughout my graduate studies. I would further like to thank the other members of my committee, Dr. Thomas Voice and Dr. Stephen Boyd, for their time and effort in the completion of this research.

Last, and certainly not least, I would like to thank Reza Rakhshandehroo for his friendship and support throughout this research. I am fortunate to have known him and I will forever remember his kindness and friendship.

TABLE OF CONTENTS

LIST OF TABLES	vii
LIST OF FIGURES	viii
INTRODUCTION	1
CHAPTER 1	
METHODS AND MATERIALS	6
Soil Samples	6
Adsorption of HDTMA	6
Cation Release	7
Soil Suspension Turbidity	7
Conductivity Experiments	8
HDTMA Distribution	11
CHAPTER 2	
RESULTS AND DISCUSSION	13
Chemistry.....	13
Hydraulic Conductivity	17
CHAPTER 3	
CONCLUSIONS.....	32
APPENDIX A	
LITERATURE REVIEW	33
Applications of Organically Modified Clays.....	33
Chemistry of HDTMA Sorption.....	34
Desorption of HDTMA	37
Hydraulic Conductivity	39
Permeant Properties.....	41
Soil Physical Properties.....	42
Effects of HDTMA on Clay Physical Properties.....	47
Soil Water	49
Effect of Normal Stresses on Soil Structure	51
Effect of Organic Permeants on Hydraulic Conductivity	52
Effect of Organomodification on Hydraulic Conductivity	55

APPENDIX B	
SUMMARY OF TERMS	59
APPENDIX C	
DETAILED METHODS AND MATERIALS	61
Consolidometer Assembly	61
Vacuum Saturation	64
Blank Conductivity Measurements	70
Soil Packing / Hydraulic Conductivity Experiments.....	77
System Dismantling.....	93
Column Sectioning for CHN Analysis	97
Turbidity Testing of Treated Soil Columns.....	100
Used Filter Paper Blank Conductivity Measurements	101
Calculations and Data Reduction	103
APPENDIX D	
ENGINEERING APPLICATION	112
LIST OF REFERENCES.....	115

LIST OF TABLES

Table 1. Soil Suspension Turbidities of Samples from Treated Soil Columns.	26
Table 2. Average HDTMA Soil Concentrations at Various Locations in Treated Soil Columns.	30
Table 1C. Values of Hydraulic Conductivity Used to Calculate Soil Conductivities from Falling Head Measurements.	107
Table 2C. Values of Hydraulic Conductivity Used to Calculate Soil Conductivities from Inlet Pressure Measurements.	109

LIST OF FIGURES

Figure 1. Profile Showing Proposed Sorptive Zone Created by Injection of HDTMA.....	3
Figure 2. Schematic of Experimental Procedure	9
Figure 3. CHN Analysis Sectioning and Numbering.....	12
Figure 4. HDTMA Sorbed, Total Cation Release, and Soil Suspension Turbidity at Various HDTMA Loadings	15
Figure 5. Relative Hydraulic Conductivity vs. Flushing Time.....	19
Figure 6. Soil Suspension Turbidities for Soil Before Experiments and After Flushing Period	21
Figure 7. Relative Hydraulic Conductivity vs. Treatment Time	24
Figure 1C. Consolidometer Assembly	62
Figure 2C. Vacuum Saturation System.....	65
Figure 3C. Load Frame and Consolidometer Configuration	72
Figure 4C. Modified Pumping System for Conductivity Experiments	86
Figure 5C. CHN Analysis Numbering.....	99

INTRODUCTION

Currently, pump and treat methods are commonly used to control the migration of groundwater contaminant plumes (Blowes *et al.* 1995). Extended operation of these technologies is often necessary to achieve clean-up goals. This approach is costly due to the continuing need for equipment maintenance, possible treatment of discharge water, and monitoring (Eykolt and Sivavec 1995). To reduce the cost of site remediation, there is a strong interest in development of alternative technologies that are more passive in operation for contaminant plume management in the subsurface (Hatfield *et al.* 1992).

In soil-water systems nonionic organic compounds (NOCs) are sorbed primarily by partitioning into soil organic matter. Soil minerals are ineffective sorbents due to the hydrophilic nature of clay surfaces and the preferential adsorption of water by polar surfaces of the other mineral components of soils (Jaynes and Boyd 1991). Therefore, low organic matter surface soils, subsoils, and aquifer materials have limited capabilities for removing NOCs from water and hence for retarding the migration of dissolved contaminants (Lee *et al.* 1989). The ultimate result is the contamination of large aquifer regions (Hatfield *et al.* 1992).

Cationic surfactants of the form $[(\text{CH}_3)_3\text{NR}]^+$ or $[(\text{CH}_3)_2\text{NRR}]^+$ (where R is an alkyl hydrocarbon) have been used to displace native inorganic cations in clay minerals (e.g. bentonites) and soil clays. In the resultant “organo-clay” an organic phase develops

on the clay surfaces and interlayers, due to the agglomeration of alkyl hydrocarbon moieties, which acts as a sorbent for low-water-solubility organic contaminants (Boyd *et al.* 1988, 1991; Lee *et al.* 1989; Jaynes and Boyd 1991; Sheng *et al.* 1996a,b). The sorptive organic phase formed by adding hexadecyltrimethylammonium (HDTMA), a large cationic surfactant, to subsoils has been shown to be 10 to 160 times more effective (on an equal weight basis) than natural soil organic matter in the sorption of NOCs (Boyd *et al.* 1988; Lee *et al.* 1989; Sheng *et al.* 1996a,b). Sorption coefficients of common groundwater contaminants were shown to increase by over two orders of magnitude in high and low clay content subsoils that were treated with HDTMA (Boyd *et al.* 1988; Lee *et al.* 1989; Sheng *et al.* 1996a,b)

Underground injection of cationic surfactants for the purpose of creating sorptive zones, also termed subsurface sorbent systems (Hatfield *et al.* 1992), *in-situ* treatment curtains (Blowes *et al.* 1995), and reactive permeable barriers (Eykholt and Sivavec 1995), has been suggested for the remediation of subsurface contaminant plumes (Burris and Antworth 1990). Injecting cationic surfactant solutions into media downgradient from contaminant plumes could be used to create a sorptive zone which would significantly retard the migration of contaminants away from the pollution source. Because of the sorptive properties of the zone, NOCs would be removed from the aqueous phase and retained by the organo-clays in the treated soil. A typical profile of such a sorptive zone is shown in Figure 1. This approach could potentially provide containment and groundwater treatment at a significantly lower cost than pump and treat operations (Eykholt and Sivavec 1995). Sorptive zone technology, coupled with biodegradation, could be used as a comprehensive soil and groundwater restoration

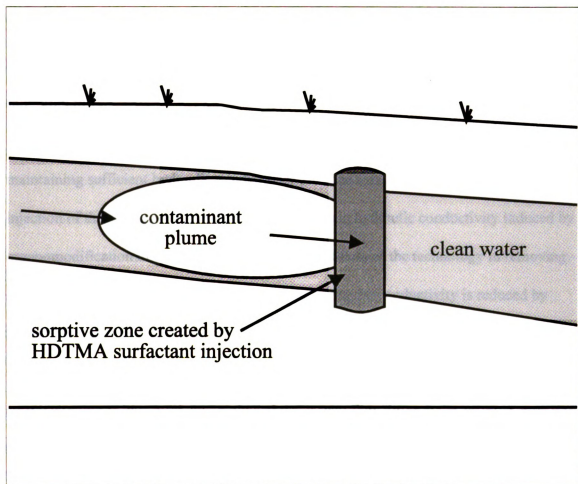


Figure 1. Profile Showing Proposed Sorptive Zone Created by Injection of HDTMA

technology (Burris and Antworth 1992; Nye *et al.* 1994; Crocher *et al.* 1995). Soil modification with large organophilic cations such as HDTMA has been shown to be highly effective (Boyd *et al.* 1991) because they very efficiently displace indigenous cations by ion exchange and are bound nearly irreversibly (Xu and Boyd 1994, 1995a). Burris and Antworth (1992) demonstrated the potential of creating a stable sorptive zone by injection of HDTMA into a model aquifer and by noting a decrease in contaminant migration rates.

Successful field application of sorptive zone technology also depends on maintaining sufficient hydraulic conductivity after the formation of the sorptive zone by injection of the surfactant (i.e. HDTMA). Changes in hydraulic conductivity induced by organomodification of soils may preclude the usefulness of the technology in removing organic contaminants from groundwater. If the hydraulic conductivity is reduced by treatment, contaminated water may flow through regions of higher conductivity (with no surfactant) adjacent to the sorptive zone. Conversely, if the hydraulic conductivity of the sorptive region is increased, contaminated water may flow through the sorptive zone too rapidly for removal of the contaminants from the aqueous phase.

There have been no studies published on changes in hydraulic conductivity induced by the creation of sorptive zones by *in-situ* injection of cationic surfactants such as HDTMA. Burris and Antworth (1992), during their study on the chemical aspects of sorptive zone creation, made the qualitative observation that no substantial changes in hydraulic conductivity were produced by *in-situ* injection of HDTMA into their model aquifer. However, the apparatus used in that study precluded precise quantification of changes in conductivity that may have resulted. In addition, the aquifer material was not

subjected to overburden stresses that would be expected in field situations and differing levels of HDTMA treatment were not considered. In their study of the adsorption of HDTMA and its effect on clay physical properties, Xu and Boyd (1995a) found that treatment of soils with HDTMA levels above the cation exchange capacity (CEC) of the soil resulted in dispersion of clay aggregates. They suggested that this dispersion of clay particles at high HDTMA loading levels may cause undesirable changes in the hydraulic conductivity of the sorptive zone.

The objectives of this study were to (i) investigate the changes in hydraulic conductivity produced by *in-situ* treatment of soils, with HDTMA at various loadings relative to the CEC, and under different effective stresses, and (ii) understand the mechanistic basis of the observed changes in hydraulic conductivity. This information is needed to evaluate the feasibility of HDTMA sorptive zone technology and will aid in predicting changes in hydraulic conductivity that can be expected under different field situations.

CHAPTER 1

METHODS AND MATERIALS

Soil Samples

A quantity of sandy loam soil of the Oshtemo series was obtained from the B-horizon at a depth between 38 (15 in.) and 76 (30 in.) cm from a site in Hickory Corners, MI. The soil was air dried, and sieved through a US standard #20 sieve. The resulting stock soil, which was used for all subsequent experiments, was found to contain 87% sand, 10.5% clay, and 2.5% silt. The exchangeable cations of the clay fraction were determined by the MSU Soil Testing Laboratory and consisted of 83.6% Ca^{2+} , 9.1% Mg^{2+} , 5% K^{+} , and 2.2% Na^{+} , as a percentage of the cation exchange capacity. The major clay minerals, determined by x-ray diffraction analysis of Oshtemo B soil, are vermiculite, illite, kaolinite, and hydroxy-aluminum interlayered vermiculite.

Adsorption of HDTMA

Oshtemo B stock soil (2.4 g) was placed in 25 ml Corex screw top centrifuge tubes. Varying amounts of deionized water were added to each tube and 1 ml of 25 mM NaCl solution was added to adjust the ionic strength to 1 mM NaCl. Different amounts of an HDTMA stock solution (0.0225 M) were added to each tube in amounts estimated to cover the range from 0.1 to 2.5 times the CEC. The total volume of liquid added to each tube was 25 ml. The stock solution contained HDTMA-Cl (Aldrich Chemical Co.)

and ^{14}C labeled HDTMA-I (American Radiolabeled Chemicals, St. Louis, MO) in a ratio of 1000:1 to 10000:1.

Tubes were placed on a rotating shaker, allowed to mix for 4 days, and then centrifuged at 8000 rpm for 10 min. Samples of the aqueous phase were pipetted from 1 cm below the liquid surface and mixed with scintillation cocktail. ^{14}C -activity in these samples and in the stock solution were determined by liquid scintillation counting. Total HDTMA sorption was determined from the difference between the total ^{14}C added to each tube and the ^{14}C activity of the equilibrated aqueous samples.

Cation Release

Identical procedures and conditions were employed to determine cation release as in the adsorption of HDTMA experiments, except that only nonradiolabeled HDTMA-Cl solution was used. Supernatant samples were taken after centrifuging and the pH was adjusted to below 2 using 1N HNO_3 . Samples were then analyzed for Na^+ , K^+ , Ca^{2+} , and Mg^{2+} by inductively-coupled plasma emission spectroscopy.

Soil Suspension Turbidity

Turbidities of soil water slurries with varying amounts of added HDTMA were determined using the same conditions and procedures as in the cation release experiments. Slurries were mixed for four days, then allowed to settle for 30 min, after which 1 ml samples of the suspension were obtained from 1 cm below the liquid surface. The turbidity of each sample was determined following dilution with distilled water when necessary to obtain readings within the range of 10 - 100 nephelometric turbidity units (NTU).

Turbidities of samples from treated soil columns were also determined after each experiment to verify the degree of dispersion or flocculation of the clays induced by treatment. Samples from each of the treated soil columns were taken from a region close to the injection inlet of the consolidometer, near the bottom of the column. A sample equivalent to 1 g of dried soil was placed in a 25 ml Corex tube and then equilibrated with 10 ml of the treatment solution (from the experiment) in a rotating mixer for 4 days. The suspension was then allowed to settle for 5 min. before measuring turbidity as previously described. This modified procedure was chosen to preserve as closely as possible the conditions of the soil columns during the treatment period.

Conductivity Experiments

Air dried Oshtemo B stock soil (130 g) was placed in a fixed ring consolidometer with a sample diameter of 6.25 cm. Valves were attached to each inlet port of the consolidometer to allow for both injection of treatment solution and determination of conductivity by falling head measurements. The soil was poured into the consolidometer and then tamped four times with a 1.47 kg weight dropped from a height of 7.5 cm. Soil samples were packed to a nominal thickness of 2.5 cm.

After packing, the entire consolidometer was placed in a dessicater and allowed to vacuum saturate with 1mM NaCl solution for at least 12 hours. After saturation, the consolidometer was placed in a standard consolidation load frame. A schematic of the experimental sequence is shown in Figure 2. During sample preparation, a modification of the conventional consolidation procedure (ASTM D2435-90) was used to rapidly load the samples to the desired effective stress. Each load increment was applied for approximately 45 minutes prior to applying the next load. Two different effective stress

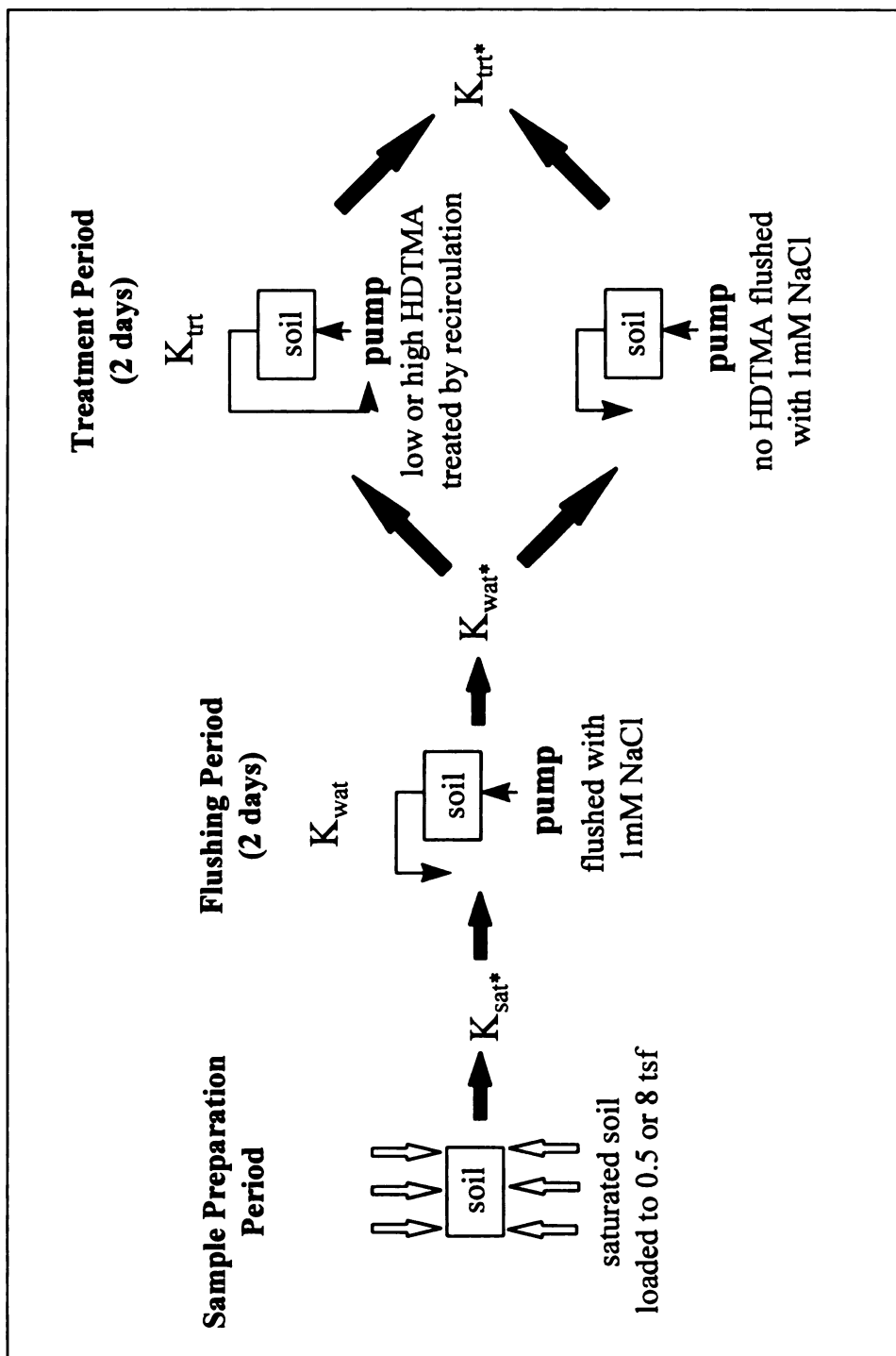


Figure 2. Schematic of Experimental Procedure

states were used in the experiments: 48 kilopascals (kPa) and 768 kPa, equivalent to 0.5 tons per square foot (tsf) and 8 tsf, respectively. These values represent depths of approximately 3m (9ft) and 44m (145 ft), respectively, based on an assumed soil unit weight of approximately 1.8 Mg/m^3 (110 lb/ft^3).

After the soil was loaded to the desired effective stress, the hydraulic conductivity (K_{sat}) was determined by falling head (ASTM D5084-90) using deaired 1mM NaCl solution. A solution of 1mM NaCl was then flushed through the sample for two days at a constant rate of 3 ml/min., using a modified high-pressure liquid chromatography pump. This pumping rate corresponds to an average linear velocity of approximately 1.4 m/day. During the flushing period, pressure readings from the inlet of the column, turbidity measurements of the collected effluent, and sample heights were recorded at regular intervals. Continuous sampling for turbidity was not used in these experiments. Therefore, relative turbidity values represented an average turbidity of the effluent over the time between readings. Values of conductivity during the flushing period (K_{wat}) were calculated from inlet pressure readings and sample heights determined from transducer readings. At the conclusion of the flushing period, the conductivity of the soil column (K_{wat}) was determined by falling head measurements.

Soil columns were then treated to a high, low, or zero HDTMA soil concentration during the two day treatment period (see Figure 2). HDTMA treatment was performed by recirculation; samples not exposed to HDTMA were flushed with 1mM NaCl. Solutions were prepared which would achieve HDTMA treatment levels calculated to be 0.8 CEC (low concentration) and 2.2 CEC (high concentration) at equilibrium. All treatment solutions were prepared with 1 mM NaCl. During the treatment period, inlet

pressures and sample heights were recorded. As in the flushing period, conductivities of the soil column during the treatment period (K_{tr}) were calculated from inlet pressure readings. At the end of the treatment period conductivity (K_{tr}) was again determined by falling head and the apparatus was dismantled. Soil samples were then taken from the soil column for turbidity measurements, as previously described. The endpoint measurements of conductivity by falling head (K_{sat} , K_{wat} , and K_{tr}) were used to verify the conductivities during flushing or treatment calculated from the inlet pressure readings (K_{wat} and K_{sat}). All conductivities reported represent conductivities of soil columns and were corrected for temperature to 20°C.

HDTMA Distribution

To determine approximate levels of HDTMA achieved by the column treatment and to determine the uniformity of treatment, soil samples were analyzed for carbon content using an elemental analyzer. After treatment, the soil columns were sectioned into 32 individual samples, as shown in Figure 3. Each sample was placed in a separate glass vial and allowed to air dry for at least one week. Nine of the samples, from regions of the soil column expected to contain maximum and minimum concentrations of HDTMA, were chosen for analysis. The nine samples chosen are shown in bold numbers in Figure 3. Percentages of carbon, on a mass basis, of the chosen samples were determined by analysis using 6 replicates of approximately 6 to 10 mg each. HDTMA soil concentrations were calculated from the difference between treated and untreated soils. Sorption isotherm data were used to correct the soil concentrations for the amount of HDTMA expected in the treatment solution at the end of each experiment.

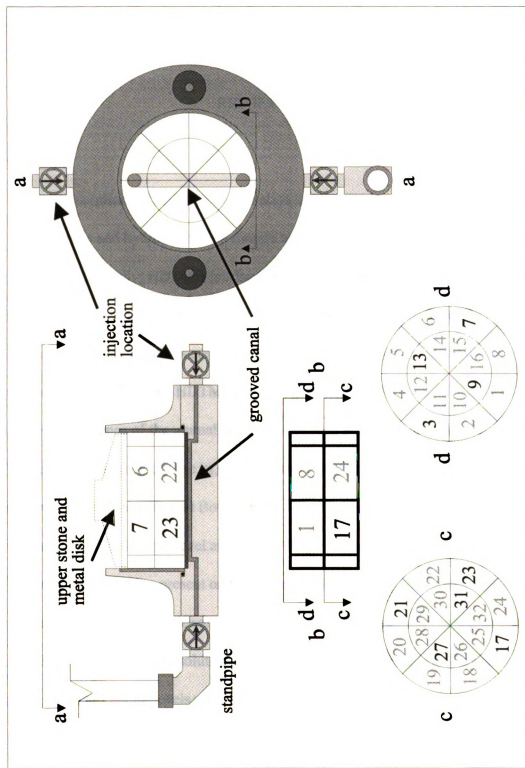


Figure 3. CHN Analysis Sectioning and Numbering

CHAPTER 2

RESULTS AND DISCUSSION

Chemistry

Adsorption of HDTMA by soil clays takes place by two primary mechanisms: ion exchange and hydrophobic bonding (Zhang *et al.* 1993; Xu and Boyd 1994, 1995a,b). Generally, HDTMA is adsorbed by ion exchange on various soils when added in quantities less than or equal to the CEC of the soil (Jaynes and Boyd 1991). After all accessible inorganic cations are exchanged by HDTMA, hydrophobic bonding is responsible for additional HDTMA sorption (Xu and Boyd 1994). Hydrophobic bonding is the consequence of the mutual attraction between alkyl chains of HDTMA cations held by cation exchange and those in solution, and the tendency of the hydrophobic tails to be removed from water (Xu and Boyd 1995a). The fraction of HDTMA adsorbed by ion exchange and the loading level at which hydrophobic bonding commences is influenced by the inorganic cation present on the exchange sites and by the electrolyte concentration of the HDTMA solution. Xu and Boyd (1995a) found that for Na⁺ saturated Oshtemo B soils in low ionic strength solutions (1mM NaCl), ion exchange was the dominant mechanism at loading levels up to the CEC of the soil, verified by the fact that HDTMA adsorption resulted in equivalent Na⁺ release. For Ca²⁺ saturated soils and for Na⁺ saturated soil at high ionic strength (>5mM NaCl), ion exchange was dominant to approximately 0.7 CEC, again verified by stoichiometric cation release. HDTMA

adsorption continued beyond this point by both mechanisms. High ionic strength in solution and divalent exchangeable cations on the clays caused hydrophobic bonding to become a dominant adsorption mechanism at HDTMA loading levels below the CEC by causing clay flocculation and thereby limiting the accessibility of inorganic exchange cations to HDTMA to more internal exchange sites of clay aggregates (Xu and Boyd 1994).

HDTMA sorption from water by the Oshtemo B stock soil in batch soil slurries is shown in Figure 4. Also shown is total inorganic cation release (Ca^{2+} , Mg^{2+} , Na^+ , and K^+) and turbidity of the solutions at the various HDTMA equilibrium liquid concentrations. Points where no HDTMA was added to the soil are plotted as an HDTMA liquid concentration of 1×10^{-5} mM. Based on cation release, it can be seen that a total of approximately 27 mmol/kg of indigenous inorganic cations could be replaced by HDTMA under the experimental conditions employed. This value was used to approximate the CEC of the Oshtemo B soil. As can be seen from Figure 4, total cation release closely followed HDTMA sorption to a loading level of 0.8 CEC (i.e. HDTMA soil concentration 22 mmol/kg), indicating ion exchange as the dominant mechanism. Above 0.8 CEC, total cation release was less than HDTMA sorbed, indicating that hydrophobic bonding contributed to additional HDTMA adsorption. These results agree well with previous findings of Xu and Boyd (1995a) who observed that hydrophobic bonding began at approximately 0.7 CEC, for Ca^{2+} saturated Oshtemo B soils.

Turbidity was initially low and remained low until the HDTMA loading level exceeded approximately 0.8 CEC (Figure 4). At HDTMA loading levels above 0.8 CEC turbidity rapidly increased and then leveled off at HDTMA liquid concentrations above

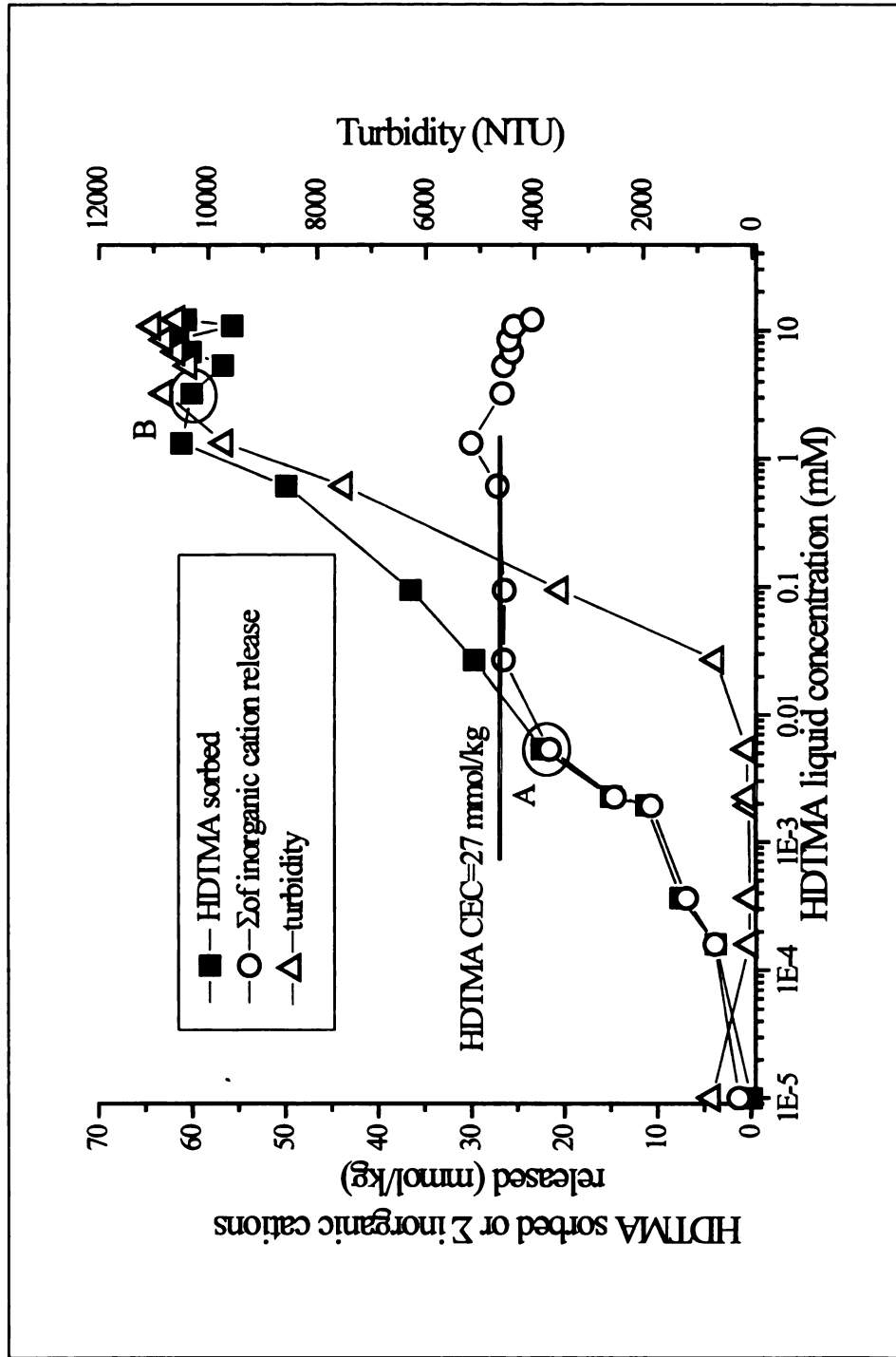


Figure 4. HDTMA Sorbed, Total Cation Release, and Soil Suspension Turbidity at Various HDTMA Loadings

1mM. Xu and Boyd (1995a), through the use of optical density and electrophoretic mobility measurements, deduced that different levels of HDTMA treatment cause differences in clay dispersion. They found that Na^+ saturated soils are initially well dispersed before HDTMA is added and then become flocculated as HDTMA loading increases to 0.5 CEC. The adsorption of HDTMA on the surfaces of the clays neutralizes the repulsive, negative charge of the clay particles. This, and the mutual attraction of hydrophobic tails of HDTMA promote a face to face association of the clay particles and result in flocculation of the clay platelets (Xu and Boyd 1994). At loading levels above 1.0 CEC the charge on the clay surface becomes positive due to the additional ammonium head groups of the hydrophobically-bonded HDTMA. The resultant charge repulsion causes the clays to redisperse and turbidity increases. Consistent with these findings, the turbidity of the soil used in this study at low HDTMA loading levels was very small (Figure 4) because clays were predominantly flocculated in a face to face association due to the presence of Ca^{2+} as the predominant exchangeable cation (83.6%) and turbidity increased rapidly at approximately the same point where hydrophobic bonding commenced.

For the soil column studies, two HDTMA loadings were selected to represent the two extremes in clay dispersion that could result from treating the soil to different HDTMA soil concentrations. The first HDTMA loading (labeled A in Figure 4) corresponds to 0.8 times the CEC, where cation exchange was the dominant HDTMA adsorption mechanism, and clay particles were well aggregated. The second HDTMA loading (labeled B in Figure 4) is equivalent to 2.2 times the CEC. At this point,

HDTMA adsorption via hydrophobic bonding was the predominant bonding mechanism causing clay dispersion.

Hydraulic Conductivity

In this study, hydraulic conductivity of Oshtemo soil, treated by recirculation of HDTMA, was investigated as a step toward evaluating the hydraulic feasibility of developing sorptive zones *in-situ*. Hydraulic conductivity (K) is a macroscopic property that is related to the soil matrix geometry and properties of the permeating liquid by the following equation (Shackelford 1994):

$$K = k \frac{\gamma}{\mu} \quad (1)$$

The intrinsic permeability k describes the matrix geometry and unit weight (γ) and absolute viscosity (μ) are the important fluid properties. The Hagen-Poiseuille equation can be employed to show the following dependence of intrinsic permeability on porosity (n) and effective pore radius (r) (Allred and Brown 1994):

$$k = nr^2 \quad (2)$$

The effective pore radius is a macroscopic parameter that incorporates the effect of pore radius, stratification, packing, arrangement of grains and pore size distribution (Wallace *et al.* 1995).

Differences in hydraulic conductivity may result from changes in either the soil matrix geometry or the fluid properties. Externally applied loads may cause consolidation or compression of the soil, resulting in a decrease in the intrinsic permeability brought about by changes in porosity and/or effective pore size. Alternatively, external stresses may be held constant and changes in hydraulic conductivity can be induced by changing

the fluid properties of the permeating liquid or by changing liquids. The introduction of different liquids creates the opportunity for the additional effects of chemically induced changes in the soil matrix geometry that are brought about primarily by the reaction of soil clays to the permeant (Shackelford 1994).

Prior to the treatment period, water saturated soil columns were loaded to the desired effective stress and then flushed for two days with 1mM NaCl to establish a stable baseline condition prior to treatment with HDTMA (Fig. 2). Typical curves of relative hydraulic conductivity during the 2 day flushing period are shown in Figure 5. Relative conductivity is the conductivity measured during flushing (K_{wat}) normalized by the conductivity measured prior to flushing (K_{sat}). Also shown in the figure are the turbidity values of the effluent measured during the same two day flushing period, shown relative to the highest turbidity recorded during that period. It can be seen from Figure 5 that decreases in relative hydraulic conductivity were associated with increases in relative turbidity.

The Oshtemo B soil used in our experiments was highly disturbed and the clay content was relatively low (10.5%). Therefore, it seems likely that the soil clays resided mostly in the pore spaces created by the sand grains with some of the clays lightly coating the sand and silt particles. The positioning of clays within the pore space created by larger particles is supported by Kenney *et al* (1992) who asserted that in well compacted mixtures of bentonite clay and sand, containing small percentages of bentonite (~10%), sand particles formed the load bearing soil matrix and that bentonite was contained in the void spaces formed by the sand particles. Less than 1% change in the porosity of our soil columns was observed during the flushing period (data not shown).

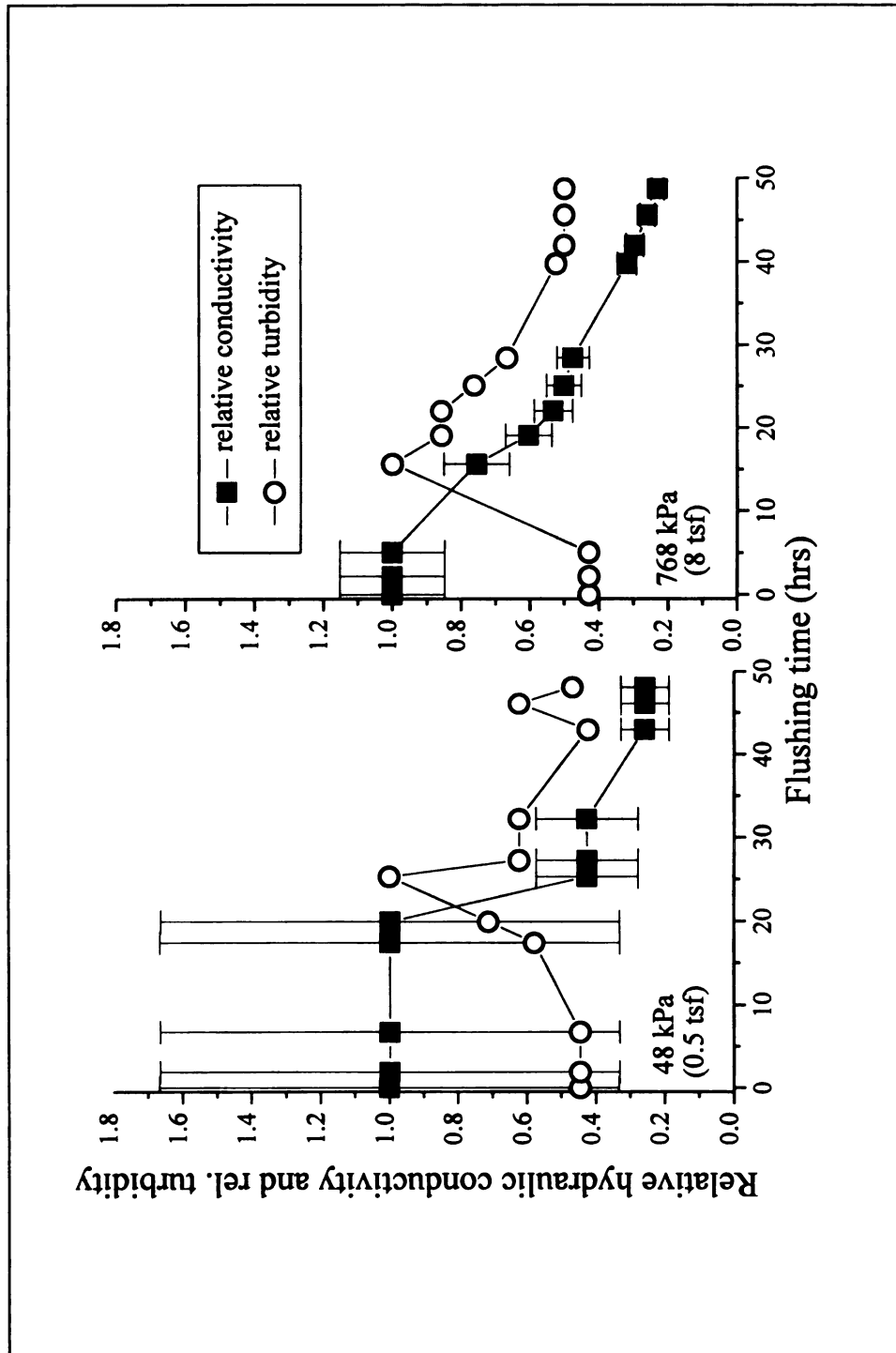


Figure 5. Relative Hydraulic Conductivity vs. Flushing Time

Therefore, based on Eq. 2, the majority of the change in intrinsic permeability, and therefore hydraulic conductivity, was due to changes in the effective pore size of the soil matrix induced by flushing the soil columns with the 1mM NaCl solution. Changes in the effective pore size were likely related to changes in the matrix produced by the behavior of clay particles.

The results shown in Figure 5 indicate that the reduction in effective pore size was likely related in part to clay migration and subsequent pore clogging. Fines migration as a cause of the decrease in relative hydraulic conductivity is suggested by the time dependent rise in the relative turbidity of the effluent solution during the flushing period, and its correspondence to the onset of decreases in relative hydraulic conductivity. Rearrangement of soil fines likely occurred due to the disturbed nature of the soil and due to the relatively large hydraulic gradient, between 4 and 40, employed during flushing. This is consistent with previous research showing that redistribution of soil fines can be induced by hydraulic gradients produced by pumping (Goldenberg *et al.* 1993). As colloids are dislodged from the soil matrix, and possibly later entrapped in pores, there is a continuous change in pore structure and subsequently a continuous change in hydraulic conductivity (Govindaraju *et al.* 1995).

A soil column was sacrificed after the two day flushing period and the turbidity of this soil at various HDTMA loadings was determined (Figure 6). The turbidity vs. HDTMA loading level relationship for the stock soil, which had not been flushed with the NaCl solution, is also shown in Figure 6. Turbidities measured when no HDTMA was added are plotted at an HDTMA liquid concentration of 1×10^{-5} mM. These relationships suggest that exposure of the soil to 1mM NaCl solution during the sample preparation

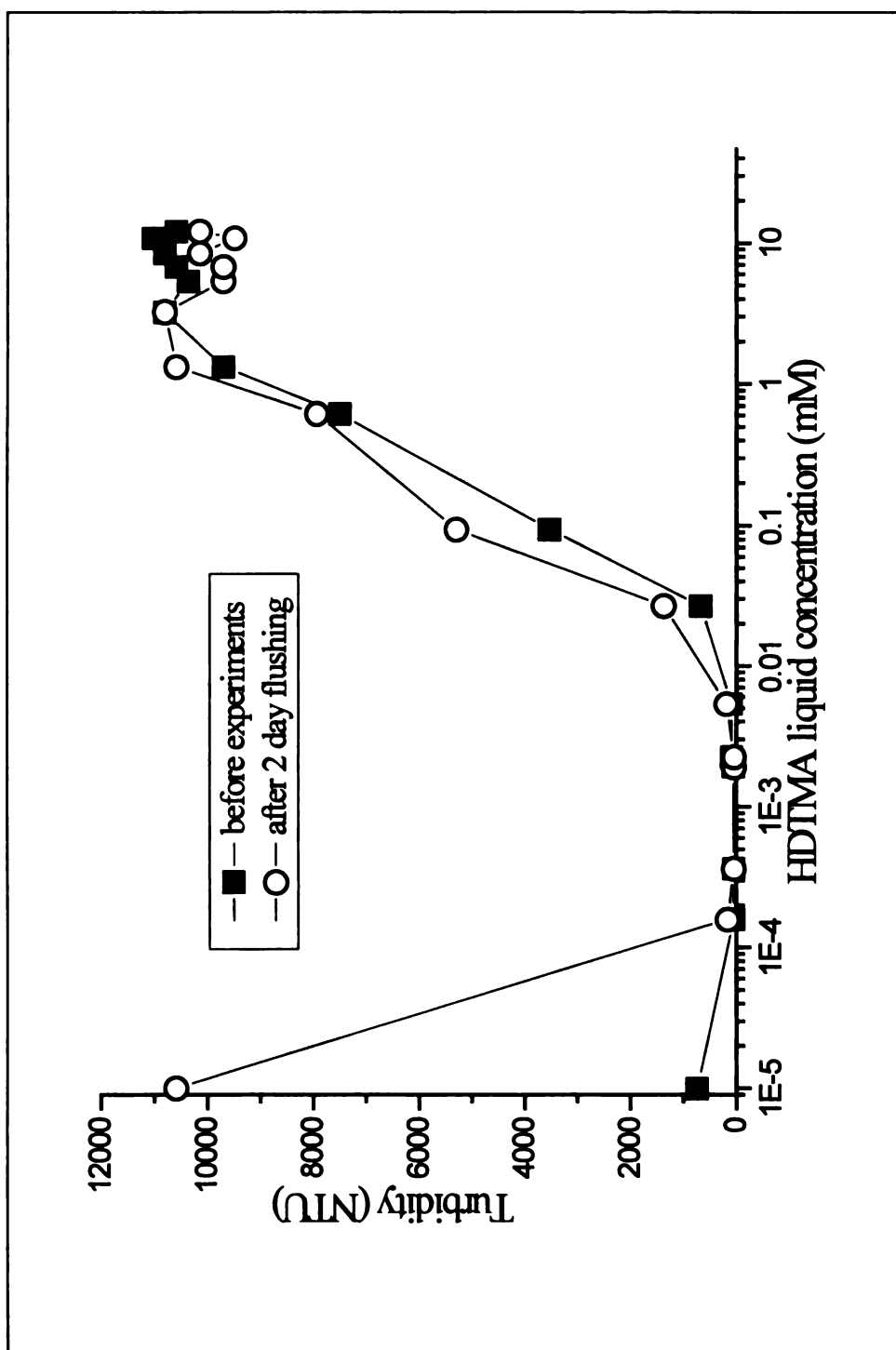


Figure 6. Soil Suspension Turbidities for Soil Before Experiments and After Flushing Period

and flushing periods dispersed the soil clay. This was made evident by the high turbidity of the 1mM NaCl flushed soil before HDTMA was added. As the HDTMA loading was increased the initially-dispersed clays of the 1mM NaCl flushed soil flocculated and then redispersed. This resulted in a U shaped curve relating turbidity to HDTMA loading (Figure 6) that is similar to the one presented by Xu and Boyd (1995a) for Na⁺ saturated Oshtemo soil. This suggests that during saturation and the two day flushing period, the exchangeable cations initially present on the clay surfaces, primarily Ca²⁺, were exchanged with Na⁺ from the saturation and flushing solution. The Na⁺ induced dispersion of the clays likely added to the amount of fines that became mobile during the flushing period. Therefore, the decrease in relative hydraulic conductivity observed during the flushing period (Figure 5) could be attributed to particle migration due to both the disturbed nature of the soil and the dispersion of the soil clays caused by the chemical characteristics of the flushing solution. This is consistent with previous experiments conducted in various porous media systems containing colloidal sized particles where Ca²⁺ replacement with Na⁺ was shown to cause the dispersion of colloids which resulted in significant colloid release and transport (Roy and Dzombak 1995). Levy *et al* (1990) linked the dispersion and transport of clays to observed decreases in hydraulic conductivity using mixtures of quartz sand (0.075-0.30 mm) and kaolinite clay that were dispersed with the dispersing agent sodium hexametaphosphate. Allred and Brown (1994) extended this understanding by showing that anionic and amphoteric surfactants produced decreases in hydraulic conductivity which they attributed to clay dispersion and pore blocking.

In addition to the pore blocking attributed to particle migration, dispersed clay particles that were not transported by fluid movement may have contributed to the decrease in conductivity observed during the flushing period. This phenomenon was static in nature, in that the clays were not transported to new locations. These clays likely sub-divided the available pore space into smaller units without migrating within the soil column. This likely contributed to the reduction in the effective pore size, and therefore, the reduction in relative hydraulic conductivity.

Following the flushing period, soil columns were treated for two days with HDTMA by recirculation, or alternatively, were continually flushed with 1mM NaCl solution (Figure 2). Relative hydraulic conductivities during the treatment period for high, low, and no HDTMA treatment are shown in Figure 7. Values of hydraulic conductivity during the treatment period (K_{tr}) were normalized to conductivity values measured by falling head after the two day flushing period (K_{wat}). As can be seen, treatment of the soil to a high HDTMA concentration resulted in the most rapid decrease in relative hydraulic conductivity and the greatest total decrease by the end of the treatment period. Low HDTMA treatment initially caused a decrease in relative hydraulic conductivity similar to or slightly greater than no treatment, but ultimately resulted in the highest relative hydraulic conductivity. Kinematic viscosity of HDTMA solutions, determined using Cannon-Fenske Routine viscometers (ASTM D 446-89a), varied less than 3% from that of the 1mM NaCl solution. In addition, porosity changed less than 1% during the treatment period. Therefore, as in the initial NaCl flushing period, changes in relative hydraulic conductivity were due primarily to changes in the effective pore radius.

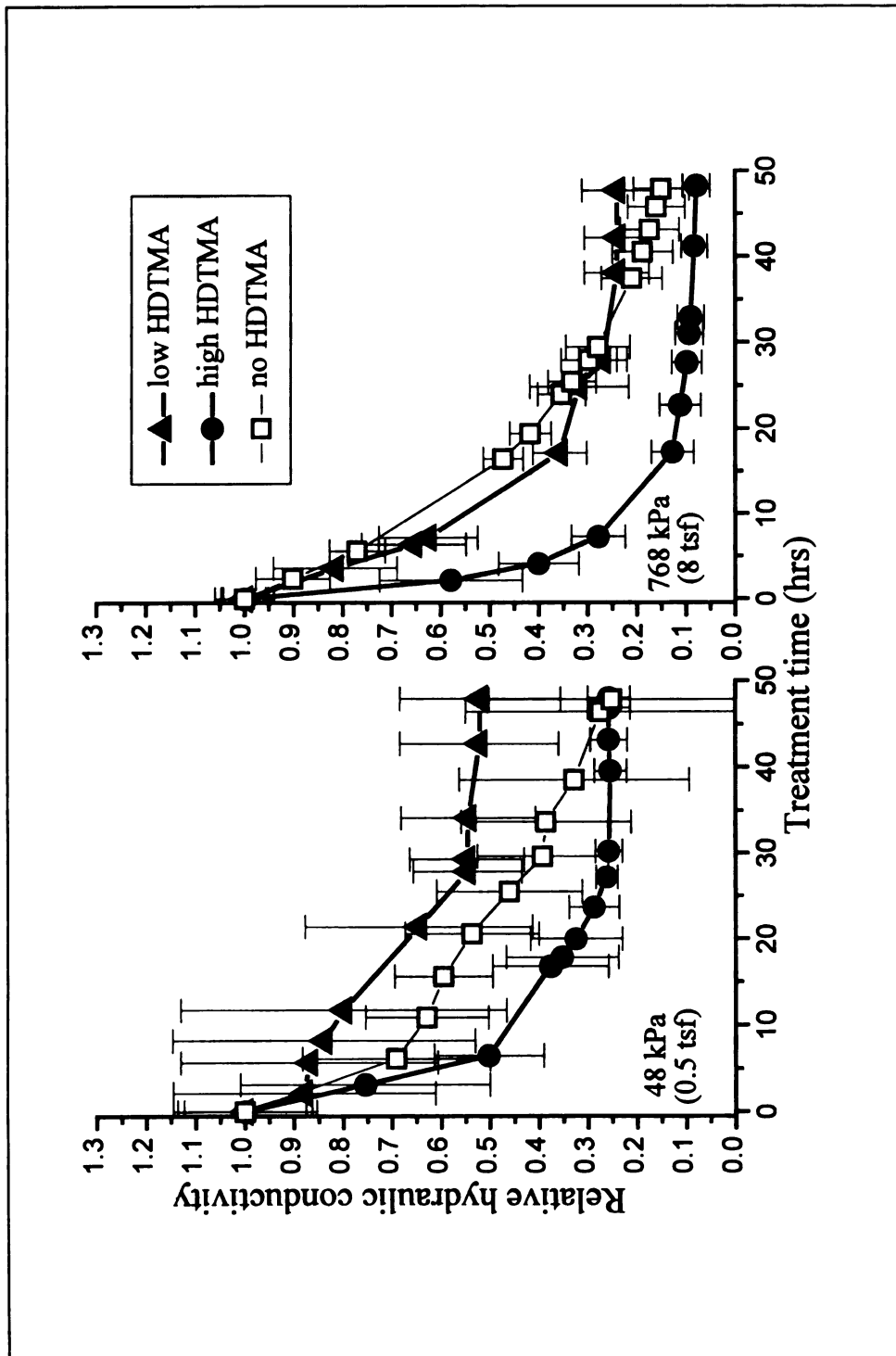


Figure 7. Relative Hydraulic Conductivity vs. Treatment Time

Columns that were not exposed to HDTMA, but rather were continually flushed with 1mM NaCl solution, experienced relatively steady conductivity decreases throughout the treatment period. Turbidity measurements on this soil indicated that no additional dispersion of clay particles took place during the treatment period (data not shown). This suggests that the exchange of Na^+ for the natural cations (e.g. Ca^{2+} , Mg^{2+} , K^+) was near equilibrium and the clays were dispersed after the initial two day flushing period. Therefore, the relative hydraulic conductivity decrease of the columns not exposed to HDTMA were most likely due to particle migration and subsequent pore clogging, attributable to the dispersed nature of the clays. Because more than 250 pore volumes of fluid were delivered during the two day flushing, it is likely that most of the changes in soil structure due to the use of disturbed soils took place in this period. Therefore, the relative hydraulic conductivity decrease shown in Figure 7 may be presumed to be analogous to decreases that would be expected in field situations where soil clays are initially dispersed and where solutions without HDTMA are pumped through the soil under high hydraulic gradients.

Soil suspension turbidities determined after the treatment period (Table 1) indicate the high HDTMA treatment concentration (point B in Figure 4) was sufficient to cause more clay dispersion than in the no treatment columns. It appears that in the no treatment columns 1mM NaCl was not sufficient for Na^+ to completely displace the predominant divalent cations, i.e. Ca^{2+} and Mg^{2+} , and hence the clays were not fully dispersed. When the soil columns were exposed to the high HDTMA treatment solution, additional dispersion occurred, relative to the no treatment case. This was because

Table 1. Soil Suspension Turbidities of Samples from Treated Soil Columns

HDTMA treatment condition*	48 kPa (0.5 tsf)	768 kPa (8 tsf)
no	⁺ 8379±1764	8489±311
low	1228±861	994±579
high	11613±509	11907±882

*High and low treatment correspond to 0.8 and 2.2 times the soil cation exchange capacity, respectively.

*All turbidities were determined after the treatment period for suspensions of soils combined with their treatment solutions. Averages were determined from three triplicates and include two standard deviations

HDTMA is far more effective than Na^+ at displacing Ca^{2+} and Mg^{2+} and fully saturates the cation exchange sites (Xu and Boyd 1994;1995a,b). Subsequent hydrophobic bonding of additional HDTMA to fully HDTMA exchanged soil clays results in the build up of positive surface charge and causes extensive clay dispersion. As in the no treatment case, particle migration took place and contributed to the relative hydraulic conductivity decrease (Fig. 7). But, because a greater degree of clay dispersion was induced by the high treatment concentration, more clays were initially dislodged from the soil matrix and were transported by the flow. Therefore, the rate of relative hydraulic conductivity decrease was initially more rapid than in the no treatment case. Likewise, some additional reduction in the effective pore radius likely took place in areas where clays did not move, or had already been deposited, due to the increase in clay dispersion. Later in the treatment period, the relative hydraulic conductivity decrease slowed as the clays reached more stable positions and no additional movement or pore clogging took place.

In general, columns that were treated to low HDTMA soil concentrations (point A in Figure 4) experienced an initial decrease in conductivity similar to or slightly more rapid than in the no treatment case and a slower decrease than the high treatment case. Due to HDTMA sorption kinetics and the high HDTMA concentration at the beginning of this treatment, a portion of the HDTMA was initially adsorbed by hydrophobic bonding. This likely caused clay dispersion and an initial decrease in conductivity similar to the no treatment case. Apparently, with time, the metastable HDTMA initially adsorbed by hydrophobic bonding (Xu and Boyd 1994), rearranged itself and became bound in a more stable state to ion exchange sites. Xu and Boyd (1994) observed this directly in kinetic studies of HDTMA adsorption where, at HDTMA levels below the

CEC, the amount of HDTMA adsorbed initially exceeded the amount of Na^+ released, but eventually they became equivalent. The eventual flocculation of clays, caused by the rearrangement of HDTMA to ion exchange sites in the column, was verified by the low average turbidities observed at the end of treatment for low HDTMA treated soils (Table 1). As a result of clay flocculation, progressively fewer clays were transported by the flow, and the more aggregated clay particles resulted in larger pores. The net effect was that the rate of relative hydraulic conductivity decrease approached zero at later treatment times and the low HDTMA treated soils were more conductive than either the no treatment or high HDTMA treated soils.

The turbidity values shown in Table 1 for the soil columns exposed to HDTMA are consistent with the final relative hydraulic conductivities shown in Figure 7. Those treatment conditions which resulted in more clay dispersion caused a greater decrease in average relative hydraulic conductivity by the end of the treatment period. Therefore, turbidity measurements may serve as a good qualitative predictor of total conductivity decreases which may result from treatment with HDTMA by *in-situ* injection.

Comparison of relative hydraulic conductivity curves of the high and low treatment cases (Figure 7) indicates that the total average relative hydraulic conductivity decrease was greater and was initially more rapid in soil columns under greater effective stress. Because the porosity of soil columns under the 768 kPa (8 tsf) effective stress was smaller, the velocity of the fluid through the pores was greater. Higher velocities likely resulted in more rapid particle transport and more particle migration overall. In addition, the smaller pore space and more tortuous flow paths in columns under the 768 kPa (8 tsf) effective stress likely resulted in more pore blocking over time.

The magnitude of differences in relative hydraulic conductivity decrease among treated and nontreated soils were small (Figure 7). In all comparisons, total decreases differed by less than a factor of three. Furthermore, rates of decrease in relative hydraulic conductivity due to treatment with HDTMA became smaller and leveled off at the end of treatment, while rates of decrease due to no treatment did not. This suggests that total relative hydraulic conductivity decrease in the no treatment case may exceed losses in hydraulic conductivity in either of the treatment cases with longer treatment time, i.e. that pumping fluid itself may have a bigger effect on hydraulic conductivity than treatment with HDTMA. These results support the hydraulic feasibility of sorptive zones created by *in-situ* injection in soils with clays which are dispersed prior to treatment.

After the treatment period, all columns exposed to HDTMA were sectioned and the HDTMA soil concentrations were determined by total carbon analysis (Table 2). As expected, the high HDTMA treatment resulted in a higher concentration of HDTMA on the soil. The differences in HDTMA soil concentration between the high and low HDTMA treatments were large enough to be statistically significant. The concentrations also agreed fairly well with concentrations expected, based on the sorption isotherm (points A and B, Figure 4). The expected HDTMA soil concentrations were 22 mmol/kg and 60 mmol/kg in the low and high HDTMA treatment cases, respectively.

The distribution of HDTMA in the columns was not always uniform. HDTMA soil concentrations in the inner region of the upper half of the column (samples 9 and 13, Table 2) were much lower than the outer region in the low treatment level case under both effective stresses. The differences were likely due to flow paths induced by the apparatus. The fixed ring consolidometer system, as shown in Figure 3, consisted of an

Table 2. Average HDTMA Soil Concentrations at Various Locations in Treated Soil Columns

HDTMA treatment condition*	top, outer		top, inner		bottom, outer			bottom, inner	
	3	7	9	13	17	21	23	27	31
48kPa (0.5 tsf) low	20.8 ± 3.4	22.6 ± 4.7	5.15 ± 2.4	7.12 ± 2.2	37.6 ± 5.9	33.1 ± 5.7	36.5 ± 4.3	27.4 ± 5.8	31.5 ± 4.6
768kPa (8 tsf) low	22.1 ± 4.0	24.3 ± 4.5	8.7 ± 3.3	6.0 ± 2.3	36.7 ± 5.7	36.3 ± 7.2	35.1 ± 3.4	29.7 ± 6.0	26.9 ± 4.5
48kPa high	67.1 ± 9.8	64.1 ± 7.3	59.8 ± 6.5	61.3 ± 7.7	64.2 ± 8.6	68.1 ± 9.9	67.1 ± 8.3	63.9 ± 8.3	57.5 ± 7.1
768kPa high	65.2 ± 8.8	65.5 ± 8.6	67.6 ± 7.9	64.1 ± 7.2	69.4 ± 8.7	63.7 ± 7.6	72.4 ± 10.1	60.4 ± 6.0	61.0 ± 7.0

*High and low treatment correspond to 0.8 and 2.2 times the soil cation exchange capacity, respectively.

+ All concentrations are expressed as a percent on a weight to weight basis and include two standard deviations.

injection inlet on one side of the consolidometer coupled with a grooved canal under the lower porous stone. The outlet was comprised of an upper stone attached to an upper metal disk, both of which were slightly smaller than the walls of the consolidometer. This configuration would have encouraged flow from along the canal which ran down the center of the bottom of the consolidometer to the exit located between the walls of the consolidometer and the perimeter of the upper stone and metal disk. The higher HDTMA treatment concentration seemed to mask this effect.

CHAPTER 3

CONCLUSIONS

Treatment of soils with dispersed clays by *in-situ* injection of HDTMA surfactant for the purpose of creating sorptive zones appears hydraulically feasible under the experimental conditions used in this study. No drastic increases or decreases in conductivity were observed subsequent to treatment at any level under the effective stresses considered. The decreases in relative conductivity observed were attributable to changes in the effective pore size, which were related to clay transport and subsequent pore blocking, and to pore space partitioning due to clay dispersion. The amount of clay migration and pore blocking that took place was dependent on the degree of clay dispersion that existed while flow occurred. Treatment of soils to higher HDTMA soil concentrations resulted in more clay dispersion, which caused more clay migration and pore space partitioning. Therefore, a larger and more rapid decrease in relative conductivity resulted. The opposite was true in the low HDTMA treatment case. The total conductivity decreases observed in the treatment cases agreed well in relative terms with turbidity measurements taken on soils after treatment. Therefore, turbidity measurements performed on soils at various HDTMA loading levels may provide a good qualitative prediction of conductivity changes that can be expected consequent to treatment.

APPENDICES

APPENDIX A

APPENDIX A

LITERATURE REVIEW

Applications of Organically Modified Clays

The study of organoclays is not a new area of research. The investigation of clay-organic interactions began over 50 years ago. An early study reacted organic bases and their salts with montmorillonite clays and presented evidence of an ion exchange reaction. Other early experiments showed that naturally occurring cations could be replaced by organic cations and that uncharged polar compounds could enter the interlayer region without the release of cations. It was also found that bentonite, after reaction with certain organic compounds gained the property of swelling and dispersing in organic fluids (Evans *et al.* 1989).

Presently, organically modified clays are being used, or have been used, in water treatment applications and for spill control. In water treatment, aqueous solutions are filtered through the clays and organic contaminants are preferentially sorbed into the organic phase of the modified clays. For spill control, modified clays have been dispersed into water and the organics are then adsorbed and held within the crystalline structure of the clays for cleanup and disposal (Alther *et al.* 1990). The clay minerals most commonly used include smectite (mainly montmorillonite and hectorite) and attapulgite. Other proposed applications of organically modified clays include waste stabilization, tank farm liners, hazardous waste liners (Evans *et al.* 1989), and sorptive

zones for hazardous waste remediation (Burris and Antworth 1990; Boyd *et al.* 1991; Burris and Antworth 1992; Xu and Boyd 1994).

There are a variety of commercially produced organo-clays which are manufactured by primarily two methods. In the wet process, the unmodified clay is placed in a slurry and is centrifuged to remove inert, nonclay materials. The supernatant is then reacted with the organic compound and the mixture is filtered, dried, and ground. In the dry process, limited amounts of moisture are first added to the clay. The clay is then reacted with the organic compound and the mixture is dried and ground (Evans and Pancoski 1989; Alther *et al.* 1990; Evans *et al.* 1989).

Surfactants are most commonly used to make organoclays. Surfactants are comprised of both hydrophobic and hydrophilic components (Allred and Brown 1994). They are surface active agents which reduce the interfacial tension of liquids and which greatly reduce the strength of the water menisci of a water compacted clay in contact with insoluble liquid hydrocarbons (Quigley and Fernandez 1989). For application to sorptive zone technology quaternary ammonium surfactants offer several advantages. They possess a positive charge that is not pH dependent and they are commercially available at a relatively low cost (Boyd *et al.* 1991).

Chemistry of HDTMA Sorption

Hexadecyltrimethylammonium (HDTMA) is a quaternary ammonium cationic surfactant with the formula $[(CH_3)_3N(CH_2)_{15}CH_3]^+$ (Boyd *et al.* 1991). HDTMA is usually added to soils in the form of a quaternary ammonium salt, including a central nitrogen atom joined to four organic groups along with an acid radical (Evans *et al.* 1989). There has been much research performed on the adsorption chemistry of HDTMA

on soil clays in batch experiments. Generally HDTMA is strongly adsorbed on clays. Over 99% of HDTMA, added to montmorillonites, was adsorbed when the amount of HDTMA added was less than 0.90 CEC (Zhang *et al.* 1993). Adsorption of HDTMA takes place through primarily two mechanisms, ion exchange and hydrophobic bonding (Zhang *et al.* 1993; Xu and Boyd 1994).

The amount of HDTMA that can theoretically be adsorbed by ion exchange is quantified by the cation exchange capacity (CEC). CEC is a quantitative measure of the amount of exchangeable cations, usually Ca^{2+} , Na^+ , or Mg^{2+} , present on the soil (Evans and Pancoski 1989). Ion exchange involves the replacement of natural, inorganic cations by HDTMA in aqueous solution. The inorganic cation is held to the clay surface by the negative charge of the clay surface, caused by isomorphous substitution in the clay lattice structure (Xu and Boyd 1995a).

Hydrophobic bonding is the consequence of the mutual attraction between the alkyl chains of HDTMA molecules and the tendency of the hydrophobic tails to be removed from water (Xu and Boyd 1995a). Specifically hydrophobic bonding involves ion-dipole and ion-ion interactions in addition to van der Waals forces (Zhang *et al.* 1993). Adsorption of HDTMA by ion exchange results in a more stable surface complex than by hydrophobic bonding. Hydrophobically bonded HDTMA is more susceptible to desorption than is HDTMA adsorbed by ion exchange (Xu and Boyd 1994).

HDTMA adsorption by clays depends on the clay type, the nature of the exchangeable cations initially saturating the clay, and the ionic strength of the aqueous solution (Xu and Boyd 1995b). While clays are considered nonideal exchangers because of the coexistence of multiple types of exchange sites with various adsorption energies,

the most important difference in adsorption energy is between interlayer and external exchange sites (Xu and Boyd 1995c). Swelling clays like vermiculites, montmorillonite contain interlayer exchange sites, while nonswelling clays like kaolinite and illite do not possess internal exchange sites. The exchange sites for non swelling clays are entirely external. Thus, the adsorption mechanisms for the two types of clay are different. When HDTMA is first added to a soil, molecules are adsorbed on the external sites of the clay by both mechanisms in a fast adsorption step. The HDTMA on the external sites then slowly rearranges into clay interlayers or other internal exchange sites of swelling clays (Xu and Boyd 1994). Nonswelling clays, such as illite do not possess internal exchange sites and therefore are not affected by the slow rearrangement step.

Generally, HDTMA is adsorbed by ion exchange on various soils when added in quantities less than or equal to the CEC of the soil (Jaynes and Boyd 1991). However, the fraction of HDTMA adsorbed by ion exchange is influenced by the inorganic cation present on the exchange sites and by the electrolyte concentration of the modifying solution. Zhang *et al.* (1993) found that 95% of the exchangeable Na^+ ions (on Na^+ montmorillonite; a swelling clay) could be easily replaced by HDTMA while only 70-75% of K^+ ions (on K^+ montmorillonite) could be easily exchanged by HDTMA. Additionally, Xu and Boyd (1994) found that high ionic strength and divalent exchangeable cations on the clays caused hydrophobic bonding to become a dominant adsorption mechanism at lower HDTMA loading levels. This was a consequence of initial flocculation before addition of HDTMA. Flocculation lead to face to face association of the clay platelets and limited accessibility of HDTMA to some of the exchange sites.

Theoretically, hydrophobic bonding takes place after all accessible inorganic cations are exchanged with HDTMA. However, like ion exchange, the fraction of HDTMA adsorbed by hydrophobic bonding is influenced by electrolyte concentration and by the type of cations present on the clay surface sites. HDTMA adsorption exceeded cation release (a condition indicating hydrophobic bonding) at HDTMA loadings above 0.95 CEC for Na-montmorillonite and above 0.70 CEC for Ca-montmorillonite (Zhang *et al.* 1993). In concentrated electrolyte solutions and in cases where the cation present on the exchange sites was divalent, hydrophobic bonding is operative before all of the exchange sites are occupied by HDTMA. Hydrophobic bonding can be a competitive adsorption mechanism with ion exchange at higher ionic strengths or in divalent cation solutions (Xu and Boyd 1994).

Whether adsorbed by ion exchange or hydrophobic bonding, HDTMA adsorption is relatively fast. No difference in adsorption was observed in column studies when the injection rate was 0.5 or 50 ml/hr (Burris and Antworth 1992). Batch studies performed on the Oshtemo B soil used in the present experiments indicated that HDTMA adsorbed by ion exchange reached equilibrium in less than 10 minutes, while hydrophobically bonded HDTMA reached equilibrium in approximately the same period of time (data not shown).

Desorption of HDTMA

In order for organically modified clays to be effective in the removal of NOCs, the soil-organic complex must remain stable when permeated with water containing the contaminants. One disadvantage of hydrophobic bonding is the tendency of hydrophobically bonded HDTMA to desorb in water (Xu and Boyd 1995a). It was found

by Zhang *et al.* (1993) that the cation selectivity coefficient values for HDTMA were one order of magnitude higher in desorption than in adsorption in the presence of KCl and NaCl, indicating that the ion exchange adsorption reaction was essentially irreversible. It was also determined that desorption of HDTMA was less than 1% of the total adsorption when the added amount of HDTMA was up to 100% of the CEC of the clays. When HDTMA adsorption increased beyond 150%, desorption increased significantly in the presence of electrolyte solutions. The increase in desorption was thought to be due to desorption of HDTMA at nonexchangeable sites (hydrophobically bonded HDTMA). Over long periods of time, HDTMA adsorption actually decreased to negative values, indicating that additional adsorption was taking place, possibly due to the redistribution of HDTMA within the clay layers due to interparticle diffusion.

Hydrophobic bonding in Oshtemo C soil was found to be essentially irreversible when all HDTMA was adsorbed by ion exchange. Hydrophobically bonded HDTMA resides on the external surfaces of the clay while HDTMA adsorbed by ion exchange is located within the interlayer or interparticle space of the clay and is not in full contact with the aqueous phase. Decreasing the ionic strength of the aqueous phase after loading promoted more desorption of HDTMA adsorbed by hydrophobic bonding (Xu and Boyd 1995a).

Desorption of hydrophobically bonded HDTMA is likely to occur in field applications of sorptive zone technology. In an *in-situ* injection scheme, hydrophobic bonding is likely to occur near the point of injection due to mass loading of HDTMA solution. Column studies by Burris and Antworth (1992) showed significant migration of adsorbed HDTMA away from the injection point after substantial flushing with water

after treatment. In addition to substantial HDTMA desorption and subsequent migration in column or natural settings, hydrophobic bonding could result in the build up of positive charges on the clay's surface leading to disaggregation of the clay molecules, mobilization of the dispersed particles, and undesirable changes in the hydraulic properties of the treated zone. It may be effective to control companion ions and to lower the ionic strength of electrolytes during modification to avoid large amounts of hydrophobic bonding (Xu and Boyd 1995a).

Hydraulic Conductivity

At present, there is little literature on the effects of organomodification on the hydraulic conductivity of treated soils relative to untreated soils. Flow of liquids in and through soils can be described by Darcy's law:

$$q = K \frac{\delta h}{\delta l} \quad (1A)$$

where q is the liquid flux, K is the hydraulic conductivity (LT^{-1}), h is the total head (L), and l is the length along the direction of flow (L). Hydraulic conductivity can be expressed as shown in equation 2:

$$K = k \frac{\gamma}{\mu} = k \frac{\rho g}{\mu} = k \frac{g}{\nu} \quad (2A)$$

where k is the intrinsic permeability (L^2), γ is the unit weight of the fluid ($ML^{-2}T^{-1}$), μ is the absolute or dynamic viscosity of the liquid ($ML^{-1}T^{-1}$), ρ is the mass density of the liquid (ML^{-3}), g is the acceleration due to gravity (LT^{-2}), and ν is the kinematic viscosity of the liquid (L^2T^{-1}) (Shackelford 1994).

Another expression of hydraulic conductivity employs the Hagen-Poiseuille equation for flow in a porous media comprised of bunched capillary tubes and shows the influence of porosity, the effective pore radius, and pore fluid properties on hydraulic conductivity:

$$K = \frac{nr^2\gamma}{8\mu} \quad (3A)$$

where K is the hydraulic conductivity, n is the porosity, r is the effective pore radius, γ is the specific weight of the fluid, μ is the fluid viscosity, and 8 is a constant that is the result of the geometry of the system (Allred and Brown 1994).

Generally, there is no excepted expression for intrinsic permeability. There are empirical relationships which relate it to porosity, grain size distribution, and tortuosity of the media (Wallace *et al.* 1995). The contribution of porosity, n, to intrinsic permeability (equation 2A) can be expressed by using the analogy of Poiseuille flow through a bundle of capillary tubes:

$$k = nr_e^2 \quad (4A)$$

where r_e is an effective pore radius, a macroscopic parameter that incorporates the effect of pore radius, stratification, packing, arrangement of grains, and pore size distribution (Wallace *et al.* 1995). As can be seen by comparing equations 1A through 4A, equation 3A contains a complete breakdown of terms included in the intrinsic permeability. Equation 4A expresses intrinsic permeability in terms of porosity and effective pore radius, including the geometric constant included in equation 3A in the effective pore radius term.

Changes in hydraulic conductivity may result from changes in the physical properties of the soil (intrinsic permeability - n , r_c) or from changes in the fluid properties of the permeating liquid (ρ, μ, ν). Externally applied loads may cause the consolidation or compression of the soil, resulting in a decrease in the intrinsic permeability (by induced changes in porosity and/or effective pore size). Assuming that no additional external stresses are applied, changes in conductivity may result when the properties of the liquid permeating the soil are changed. The change of permeating liquid may also result in structural changes in the soil (and hence a change in the intrinsic permeability) due to interactions between the fluid in the pore space and the solid soil particles that are exposed to the fluid (Shackelford 1994). In addition, factors associated with forces holding water to soils must also be considered when dealing with changes in hydraulic conductivity. A complete separation of each of the individual effects on hydraulic conductivity is difficult, if not impossible, due to their interdependence. However, discussion of each group of influences is warranted to illustrate the complexity of the interactions affecting hydraulic conductivity and to form a basis of understanding to allow discussion about any conductivity differences observed in the experiments.

Permeant Properties

As can be seen from equations 2A and 3A, hydraulic conductivity is influenced by the properties of the fluid permeating the soil column and intrinsic permeability (physical properties of soil). Equations 2A through 4A are based on the assumption of a no slip boundary at the solid-liquid interface of a pore. Since organomodification with HDTMA results in clay particles that are hydrophobic rather than hydrophilic, the no-slip

assumption will not hold for a fraction of the soil exposed to the permeating fluid (assuming that it is water) in the pore space. Therefore, rigorous interpretation of changes in hydraulic conductivity with respect to pore fluid would necessitate the evaluation of viscosity in terms of a hydrophobic solid. The determination of the viscosity of permeants using the “hydrophobic solid” condition would be difficult by standard methods. The quantification of the influence of hydrophobic solid surfaces is further complicated by the difficulty in determining the fraction of the soil which is hydrophobic and is exposed to the permeating fluid. Therefore it is assumed that equations 2A through 4A are sufficient for determining hydraulic conductivity of treated and untreated soil samples and will allow separation of the influence of pore fluid properties and soil properties (intrinsic permeability). Equations 2A through 4A are commonly applied to flows of non-wetting fluids through hydrophilic solids. This case is directly analogous to the case of flow of a wetting fluid through hydrophobic solids. Therefore it is justifiable to use equations 2A through 4A for the calculation of conductivity and expression of its influences.

Soil Physical Properties

The intrinsic permeability term in equation is used to quantify the effects of the soil physical properties on hydraulic conductivity. In equation 4A, intrinsic permeability is further broken down into porosity (n), and the effective pore radius (r_e^2). Both terms are affected by the nature of the soil structure. Yang and Barbour (1992) found that alteration in hydraulic conductivity due to brine permeation was strongly related to the initial soil structure and level of confining stress.

Definitions of soil structure and fabric, and distinctions thereof, vary with the author. According to Holtz and Kovacs (1981), the structure of a soil is taken to mean both the geometric arrangement of the particles or mineral grains as well as the interparticle forces which may act between them. Fabric refers only to the geometric arrangement of the particles within the soil matrix (Holtz and Kovacs 1981; Mitchell 1976; Shackleford 1994). Yong and Warkentin (1975) used soil structure as a comprehensive term including gradation, arrangement of soil particles, porosity, pore size distribution, bonding agents, and specific interactions between particles caused by electrical forces. The arrangement of individual particles was referred to as “packing” for coarse grains and as “fabric” for fine grained soils. Based on previous research, Yang and Barbour (1992) characterized the structure of natural soils as being made of elementary particle associations (microfabric) that are positioned in a macrostructure of soil aggregates. The porosity (i.e. soil pores) consists of both intra- and interaggregate pores, which are often termed micro- and macropores, respectively. The reader is referred to Collins and McGown (1974) for additional discussion of soil structure.

The methods and terms for describing various levels of soil fabric also differ between authors. Most often discussion of fabric is in terms of clay or clay fractions of the soil. According to Shackleford (1994) there are three levels of fabric that are important for describing the flow of liquids through clay: microfabric, minifabric, and macrofabric. Microfabric refers to the arrangement of individual particles into small aggregations. Minifabric is the arrangement of several microfabric assemblages and macrofabric consists of large aggregations of micro- and minifabric. Mitchell (1976) described macrofabric as features that can be seen with the unaided eye and microfabric

as the level of particle arrangement requiring at least an optical microscope for study. Other more complex descriptions of soil particle assemblages are included in other references, but are not warranted here.

As can be seen from the preceding discussion, the description of natural soil structure is convoluted, at best. It is sufficient to consider highly disturbed soil as a natural mixture of fine particles (i.e. clay) and of coarse particles (silt and sand). These larger particles either form a skeleton with clay coating them or occurring in pores or the larger particles rest in a clay matrix (Yong and Warkentin 1975). Kenney *et al.* (1992) found that in well compacted mixtures of bentonite and sand with bentonite contents of about 10%, sand formed the load bearing matrix and bentonite was contained in the voids between sand particles. A study on the effect of gravel on the hydraulic conductivity of a compacted clay found that clayey soils containing up to 60% gravel could be compacted to achieve conductivities of less than 1×10^{-7} cm/s. Between 16% and 60% gravel the conductivities increased only marginally. Between 60% and 80%, however, the conductivity was found to increase 50 fold. Below 60% the clay and other fine particles were arranged between the structure of the gravel but no large pores developed. Above 60% the gravel became the dominant influence on hydraulic conductivity because of the existence of larger pores between gravel particles (Shelley and Daniel 1993).

Each of the aforementioned findings address the structural characteristics of a synthesized soil. However, they form a basis upon which the description of a highly disturbed natural soil can be made. Natural soils, which are somewhat well graded, can be expected to possess a much wider range of grain sizes, and therefore could be expected to result in much smaller pores than in the case of mixtures with two drastically different

grain sizes. However, natural soil that is highly disturbed can still be considered in the same way. When the clay content of the soil is relatively small (i.e. $\sim 10\%$), the larger sand particles will likely form the load bearing matrix of the soil with clays lightly coating the sand and silt particles and/or residing in the pore space created by the larger grains. Since it is a natural soil, some aggregates of clay, sand, and silt can be expected. Pore distribution is likely very similar to the definition by Yang and Barbour (1992). The pores are likely distributed between pores going through aggregates and those going between aggregates (micro and macropores, respectively). Disturbance of the soil likely results in a relatively large amount of the clay being freely distributed between the pores created by the larger grains and aggregates (i.e. macropores) and on the surfaces of the aggregates exposed to these macropores. The existence of free clay within aggregates is highly unlikely, but the possibility exists that clays within the aggregates are exposed to pore liquid. Because the flow of liquids through soils is largely governed by the flow of liquid through the macropores, there exists the potential for the clays residing in these macropores to exert a significant influence on the hydraulic conductivity of the soil. The influence of clays on the hydraulic conductivity of a soil is obviously greater at higher clay contents and diminishes greatly as the fraction of clay in a soil becomes smaller. Changes in clay structure have the potential to alter the hydraulic conductivity of soils in two ways: by changing the porosity of the soil or by changing the effective pore size.

Through extensive study of clay particle interaction in colloidal suspensions, van Olphen (1977) established several modes of clay particle association. These interactions described the microassemblage of clay particles in aqueous solutions. While these associations may be applicable to conditions in the pore solution when soil is saturated,

interactions with silt and sand as well as changes caused by deposition and compaction, may complicate the designations given. These associations, however, establish a conceptual definition of dispersed and flocculated structure of the microfabric of clays that is discussed below.

The interparticle forces of attraction and repulsion determine the clay particle arrangement, or fabric (Yong and Warkentin 1975). These forces are related to the electrical forces of the diffuse double layer. As mentioned earlier, clay particles carry a net negative charge which is balanced by exchangeable cations. When the clay particle is placed in water the cations, plus loose anions, swarm around the colloid and makes up the diffuse double layer. The swarm of cations and clay particle is termed a micelle (Lambe 1958a).

Since clay particles carry a net negative charge, they electrostatically repel. Repulsion is also caused by the adsorption of water on clay surfaces. This is manifested in the swelling properties of most clays when wetted. The repulsion becomes effective when two particles become close enough for the double layers to overlap (Guoy-Chapman theory). There are also attractive forces that act between the particles due to secondary valence forces. These forces, when combined with the repulsive forces due to electrostatic charge, constitute the total potential of the system (Lambe 1958a). When two clay particles are less than 15\AA apart there is a net attraction between the particles and the particles essentially flocculate (Yong and Warkentin 1975). Conditions which cause the double layers to become smaller allow particles to become closer together and therefore make flocculation more probable. The following conditions are conducive to flocculation:

INCREASING:	electrolyte concentration
	ion valence
	temperature
DECREASING:	dielectric constant
	size of hydrated ions
	pH
	anion adsorption (Lambe 1958a)

The chemical nature of the pore water fluid has a direct impact on the modes of particle interaction that take place between clay particles.

While these generalizations can be made when looking at primarily fine grained soils, the extension of the influence of external factors on the mode of clay particle interaction in coarser grained soils is not straightforward. As was mentioned earlier, sand and silt size particles that are present in the soil will complicate the influence of pore fluid on clay association.

Effect of HDTMA on Clay Physical Properties

Modification of soils through use of HDTMA results in an organophilic clay capable of retaining NOCs. In addition to changing the nature of the clay surface from hydrophilic to hydrophobic, organomodification also results in changes in the physical properties of the clays. The alkyl chains of HDTMA adsorbed onto the clay surface may form monolayers, bilayers, pseudotrimolecular layers or paraffin complexes, depending on the mineral charge of the clay. In higher charge, swelling clays, like vermiculites and high charge smectites, HDTMA forms paraffin complexes, interstratified mixtures of bilayers and paraffin complexes, or pseudotrimolecular layers. HDTMA does not affect the basal spacings of illite and kaolinite (non-swelling clays) (Jaynes and Boyd 1991).

Xu and Boyd (1995a) studied the effects of organomodification on the electrophoretic mobility and degree of clay dispersion of Na^+ saturated clay and Ca^{2+}

saturated clay. In general, increased HDTMA adsorption by ion exchange caused flocculation and face to face association of the Na^+ saturated clay at HDTMA loadings above 0.5 CEC (shown as decrease in solution turbidity). In the case of Ca^{2+} saturated clay, the clay was initially flocculated due to the high charge density of the clay. Therefore increased HDTMA did not affect the degree of turbidity of the clay solution. As the HDTMA adsorption approached one CEC, in the case of the Na^+ saturated clay, the electrophoretic mobility of the clays increased drastically with a small addition of HDTMA, indicating hydrophobic bonding. Hydrophobic bonding, initially shown to be occurring only on the external sites of the clay, caused the clays to disperse. The development of positive surface charges, due to hydrophobic bonding of HDTMA, prevented formation of aggregates. The behavior of Ca^{2+} saturated clay was similar, but the change in turbidity and electrophoretic mobility occurred at approximately 0.7 CEC, due to the divalent cation presence on the clay exchange sites. In general, it can be assumed that HDTMA modification of soils causes the formation of aggregates up to a loading level of 1.0 CEC, as long as no hydrophobic bonding takes place. The degree of hydrophobic bonding and the HDTMA loading level at which the hydrophobic bonding begins depends, as was mentioned earlier, on the inorganic cation present, the initial charge density of the clays, and the electrolyte concentration.

As mentioned previously, Xu and Boyd (1995a) found primarily two different types of clay association, depending on HDTMA loading level. In their terms, the flocculation of clay by adsorption of HDTMA resulted in a face to face association of the clay platelets, while dispersion at higher HDTMA adsorption (hydrophobic bonding) resulted in a disaggregation of clay aggregates. A comparison to definitions of modes of

particle association in clays suspensions given by van Olphen (1977) indicates that the dispersed condition mentioned by Xu and Boyd (1995a) is most like a “dispersed” and “deflocculated” mode of clay described by van Olphen, while the flocculated clay is more like a “aggregated” but “deflocculated” mode of clay association. Based on these conceptual definitions of clay association, it seems likely that a change in clay association, or structure, caused by adsorption of HDTMA on clay surfaces may induce a change in hydraulic conductivity. A change from a dispersed clay to a flocculated clay (in Xu and Boyd’s terms) would result in clays in the macropores coming together to form face to face associations. This would result in a larger effective pore size by creating larger channels in the macropores of the soil. Conversely, a change from flocculated to dispersed clay would result in a smaller effective pore size by partitioning the pore space (likely the macropores) into smaller flow channels.

Soil Water

The structure and properties of water in a soil are not known in detail. However, the presence of water in a soil matrix can have a profound effect on the structure and permeability of a soil (Mitchell 1976). Water does not have much effect on the behavior of granular soils. However, fine grained soils, or ones containing a significant amount of clays are strongly influenced by the presence of water (Holtz and Kovacs 1981). Therefore, the influence of water on soil structure or indirect influence on factors previously mentioned will be discussed here.

Clay particles in soils are negatively charged, long, plate shaped particles (Daniel 1994) and are always surrounded by layers of water molecules (Yong and Warkentin 1975). The water is held by several different mechanisms, mainly due to the attraction of

dipolar water to electrically charged soil and attraction of dipolar water to the cations occupying exchange sites on the clay surface (Lambe 1958a). The possible mechanisms are listed below. It should be noted that it is probable that combinations of each of these mechanisms are responsible for the water which exists on or around the clay surface.

1. Hydrogen bonding
2. Hydration of exchangeable cations
3. Attraction by osmosis
4. Charged surface - dipole attraction
5. Attraction by London dispersion forces (Mitchell 1976).

Whatever the mechanisms of attraction, water and cations in solution are held tightly enough to be termed “adsorbed” to the clay particle. This adsorbed water and cations form the diffuse double layer around the soil particle. Both the soil particle and the double layer serve to block flow paths (Daniel 1994). When interparticle spacing approaches 20\AA , all of the water between clay particles is tightly bound and no flow takes place between the particles (Lambe 1958a). The thicker the double layer or the closer the particles, the more narrow and tortuous the flow paths. This transcends to a lower permeability (Daniel 1994).

In terms of compaction, water content before initial compaction has an effect on the structure of the soil and therefore its permeability. Hydraulic conductivity of clays generally decreases with molding water content and reaches a minimum just wet of optimum. Specifically molding water content influences the arrangement of clay particles (or units of clay particles). Samples of clay compacted dry of optimum or natural clay tend toward a random orientation of particles (flocculated) and therefore would be expected to have larger hydraulic conductivities than soils compacted wet of optimum or remolded. Wet compacted samples would tend toward a more parallel

arrangement. The more parallel the clay platelets are, the smaller the average void ratio and the more tortuous the flow (Lambe 1958b).

It is not known what effect the adsorption of HDTMA has on the structure of the diffuse double layer surrounding clay particles. Because the adsorption of HDTMA results in a hydrophobic environment on the clay surface, it is unlikely that the diffuse double layer, which surrounds the clay particle, is sustained during and after HDTMA adsorption. When treated independent of the many other factors which have the potential to change conductivity, an eradication of the diffuse double layer may increase conductivity by making the spaces between clay aggregates greater (by flocculation) and by destroying the layer of static water between clay particles that exists under normal conditions. Consideration of this effect is beyond the scope of the research performed here. Therefore, it will not be discussed further.

Effect of Normal Stresses on Soil Structure

The application of external normal stress also has an effect on soil structure and therefore hydraulic conductivity. Under normal pressure, particles tend to become more parallel in arrangement (Lambe 1958a). The compaction of a saturated clay under an increase in one dimensional pressure is due primarily to the reorientation of particles and to a decrease in micelle size (Lambe 1958b). As normal pressure is applied, hydraulic conductivity would be expected to decrease due to a reduction in pore size and the formation of more tortuous flow paths.

The amount of compaction a soil undergoes depends on the initial arrangement of particles. Volume change through both particle rearrangement and compression is reduced because of optimum packing. With loose packing there is a tendency for

particles to readjust to new positions of equilibrium under external stress to attain a minimum potential energy (Mitchell 1976).

Effect of Organic Permeants on Hydraulic Conductivity

Much research has been performed on the effect of organic permeants on the physical structure of clays and on the hydraulic conductivity of clayey soils. A summary of research in this area is provided by Bowders (1985) and Mitchell and Madsen (1987). As untreated soils are exposed to organic liquids, the clays shrink and cause cracking, which significantly increases the hydraulic conductivity. Conversely, most clays can be expected to swell when permeated with water. The addition of counterions to clays (or increase in electrolyte concentration) results in adsorption to the Stern layer and a subsequent reduction in repulsive potential and thickness of the diffuse double layer (Brown and Thomas 1987). The primary interaction affecting large increases in hydraulic conductivity is shrinkage of the compacted clay upon permeation with relatively pure organic solvents having dielectric constants lower than water (Shackleford 1994). According to diffuse double layer theory, decreases in the dielectric constant of the solution permeating the clay soil causes a decrease in the diffuse double layer, causing particles to come closer together. This causes cracks and fissures to develop that increase hydraulic conductivity (Brown and Thomas 1987). The dielectric constant of a permeant decreases as the amount of hydrophobic contaminant in the aqueous phase increases. However, it was found that large increases in conductivity only occur at large organic liquid concentrations. Quigley and Fernandez (1989) found that at all concentrations of organic liquids up to 70%, the hydraulic conductivity decreased in a manner which mirrored the increase in viscosity. Above 70% ethanol entered the double layer around

the clay particles and caused contraction according to the Gouy-Chapman theory. Conductivity increases were observed to be 100 to 1000 times that of water conductivity. Aqueous solutions with organic concentrations below 70% still cause swelling, but not to the magnitude observed for water (Shackleford 1994). For swelling clays, the swelling is mostly attributable to increases in d spacing while for non-swelling clays the increase is attributable to changes in the spacing between particles (Brown and Thomas 1987).

Bowders and Daniels (1987) tested four organic chemicals for their effect on the hydraulic conductivity of compacted illite and kaolinite clays. It was found that neutral, polar methanol did not affect the hydraulic conductivity of either clay at concentrations below 80% (by volume). Heptane and TCE as pure liquids resulted in large increases in hydraulic conductivity. In general, no alteration of conductivity was observed for dielectric constants greater than 40 and substantial increases were observed for liquids with a dielectric constant less than 35. Increases were attributed to shrinkage of the double layer surrounding the clay particles. When the shrinkage occurred, macropores and cracks developed, causing an increase in conductivity.

Fernandez and Quigley (1991) studied the effect of permeation of a clayey soil with various concentrations of dioxane and ethanol, under differing effective stresses. They found that at low effective stresses, permeation of pure ethanol or pure dioxane produced large increases in hydraulic conductivity due to double layer contraction and the development of macropores and shrinkage cracks. They found that application of vertical effective stresses prior to permeation with either organic liquid eliminate the increase. A higher effective stress was needed to eliminate the increase during permeation of dioxane than was needed for permeation of ethanol. When effective stresses were applied after

the permeation, an effective stress four times larger than that needed prior to ethanol permeation, was needed to eliminate the increase in hydraulic conductivity. In the case of dioxane, effective stress application after permeation did not eliminate the hydraulic conductivity increase. This study suggests that the application of effective stresses prior to organic permeation may negate the changes in conductivity induced by a collapse of the double layer. It is likely that the same is true for changes induced by treatment of soils with HDTMA. The application of effective stresses prior to treatment of soils with HDTMA will likely dampen the magnitude of hydraulic conductivity change that is observed.

Since organically modified clays have surfaces that are hydrophobic in nature rather than hydrophilic, it is expected that treated clay soils should behave opposite untreated soils when permeated with organic liquids. The swell volume of organobentonites increased with decreasing polarity (decreasing dielectric constant) of the wetting fluid while the swell volume of untreated bentonites increased with increasing polarity (increasing dielectric constant) of the wetting fluid (Smith and Jaffe' 1994). Sai and Anderson (1992) measured hydraulic conductivities of a cement-asphalt emulsion, a bentonite clay-sand, an organophilic clay-cement, and an attapulgite clay-cement when permeated with water and then with methylene chloride. The cement asphalt emulsion experienced large increases in hydraulic conductivity when permeated with methylene chloride, possibly due to the chemical deterioration of the asphalt structure due to the methylene chloride. The bentonite-clay cement experienced hydraulic conductivity increases of two orders of magnitude compared to hydraulic conductivity with water. The organophilic clay cement showed relatively high conductivities to water (1.9 to 4.4 x

10^{-6} cm/s). When permeated with methylene chloride, the organophilic clay cement showed initial decreases in hydraulic conductivity and then conductivities similar to water after prolonged permeation.

The observations of Sai and Anderson (1992) illustrate that the behavior of organically modified clays is different than that of untreated clay when permeated with organic liquids. The explanation of the behavior, however, may not be straightforward. As mentioned before, the expected behavior of the treated soils should be opposite that of untreated soil and has been proven. However, organomodification results in the formation of a hydrophobic partition phase at the clay surface. The formation of the synthetic organic matter phase may preclude use of the diffuse double layer theory to explain the initial decrease in hydraulic conductivity experienced upon permeation with pure methylene chloride. The relatively high values of conductivity of water could be attributable to the inherent increase in viscosity caused by permeation with water and the existence of a hydrophobic, synthetic organic phase at the clay surfaces. Decreases experienced upon permeation with methylene chloride could also be caused, contrary to the diffuse double layer theory, by partitioning of some of the organic contaminant into the organic matter phase created by organomodification.

Effect of Organomodification on Hydraulic Conductivity

There has been few studies performed on the effects of organomodification on the hydraulic conductivity of treated soils. A study performed by Allred and Brown (1994) on loam and sand packed to consistent dry bulk densities showed several trends. Although the soils were not treated before permeation of the solutions, some adsorption of surfactants did take place. Maximum reductions of hydraulic conductivity occurred in

the case of ionic surfactants and was 2 orders of magnitude within 0.6 pore volumes. Most of the surfactant adsorbed was found to be at the inlet of the column. Conductivity losses were attributed to reductions in hydraulic conductivity in a layer of the soil column where most of the surfactant was adsorbed. While the surfactants could form layers on the clay that would clog smaller pores, it was thought that these layers would not greatly constrict the larger pores through which the majority of the flow took place. In addition, hydraulic conductivity reduction due to changes in the viscosity of the pore fluid could only be in the magnitude of tens of percent rather than orders of magnitude. Reductions in hydraulic conductivity were attributed to soil structure alteration due to dispersion and to the formation of pore clogging, surfactant, lyotropic liquid crystals.

Hydraulic conductivities of HDTMA modified clay, bentonite liners were found to be greater than the hydraulic conductivity of untreated bentonite liners by Smith and Jaffe' (1994). Although organobentonite liners (88% Ottawa sand, 8% untreated bentonite and 4% treated bentonite) had similar bulk and dry densities as the untreated bentonite liner when compacted in lifts in a compaction mold (88% Ottawa sand, 12% untreated bentonite), the porosities of the HDTMA bentonite was lower than that of the untreated liner (0.34 compared to 0.43). However, conductivities of the treated liner were found to be 2.81×10^{-8} while that of the untreated liner were found to be 1.96×10^{-9} cm/s (10 fold increase). In addition, complete substitution of BTEA clay for untreated clay resulted in a conductivity increase of four orders of magnitude. The increase in hydraulic conductivity was due to the inability of the organobentonite to intercalate significant amounts of water. This is because the interlayers of the clay become hydrophobic when treated. Therefore, the clay does not swell in the presence of water and does not fill the

void spaces between the larger sand grains to decrease the flow of water through the porous medium. Consequently, the organobentonite results in decreased porosity and an increase in hydraulic conductivity (Smith and Jaffe' 1994).

Wallace *et al.* (1995) measured the hydraulic conductivity of untreated and treated samples at various effective stresses. Soil samples were batch treated to 1.0 CEC of the Oshtemo B soil used. The changes in hydraulic conductivity were attributed to changes in intrinsic permeability because the pore fluid properties were found to be constant throughout the experiments. Organomodification resulted in a sample with 79% lower intrinsic permeability than the untreated sample when no normal load was applied to the sample. The initial porosity of the treated sample was 15% lower than the porosity of untreated soil, indicating that the treated sample was less able to resist the initial compaction. The difference in intrinsic permeability, however, was mainly attributed to differences in the effective pore radius (r^2 ; see equation 3). The loss of conductivity at the initial condition was the result of the smaller effective pore size of the treated soil. As the consolidation load was increased, the treated and untreated sample intrinsic permeability became the same and then at loads above 191 kPa the treated sample was more permeable than the untreated sample. The treated sample was more resistive to consolidation than the untreated sample. The observations were consistent with observations by Xu and Boyd (1995a) that clay particles treated between 0.5 and 1.0 CEC flocculate and is also consistent with the observation that the more parallel the clay particles are, the less stable and more readily remolded a soil is upon compaction. The observations were also consistent with the concept that more effectively packed samples are more resistant to consolidation and subsequent decreases in hydraulic conductivity.

Burris and Antworth (1992) modified an aquifer soil in a laboratory aquifer model *in situ* with HDTMA. They reported that no significant decrease in hydraulic conductivity took place due to treatment of the aquifer solids with HDTMA. However, the apparatus used in the experiments was not sufficient to explicitly study slight changes in hydraulic conductivity and no effective stress was applied to the aquifer model.

APPENDIX B

APPENDIX B

SUMMARY OF TERMS

This section is intended to define terms and nomenclature used in Appendix C and in the spreadsheets used for data reduction.

K_{blank}	Hydraulic conductivity of consolidometer system without soil
$K_{blank(used)}$	Hydraulic conductivity of consolidometer system without soil using filter papers from the conductivity experiments
L_{blank}	Length of stones and filter paper (1.6184 cm.)
L_{soil}	Length of soil column
L_{total}	Length of total system = $L_{soil} + L_{blank}$
L_{ref}	Length of reference puck
L_{packed}	Length of soil column after packing
L_{sat}	Length of soil column after saturation
$K_{sat}^{*}(total)$	Total system hydraulic conductivity after system saturation (immediately prior to flushing period) determined by falling head measurements
K_{sat}^{*}	Soil column hydraulic conductivity after system saturation (immediately prior to flushing period) calculated from conductivity based on $K_{sat}^{*}(total)$
$K_{wat}(total)$	Total system hydraulic conductivity during flushing period, determined from inlet pressure readings.
K_{wat}	Soil column hydraulic conductivity during flushing period calculated from $K_{wat}(total)$
$K_{wat}^{*}(total)$	Total system hydraulic conductivity after flushing period (immediately prior to treatment period) determined by falling head measurements

K_{wat*}	Soil column hydraulic conductivity after flushing period (immediately prior to treatment period) calculated from $K_{wat*}(total)$
$K_{trt}(total)$	Total system hydraulic conductivity during treatment period calculated from inlet pressures
K_{trt}	Soil column hydraulic conductivity during treatment period calculated from $K_{trt}(total)$
$K_{trt*}(total)$	Total system hydraulic conductivity after treatment period determined from falling head measurements
K_{trt*}	Soil column hydraulic conductivity after treatment period calculated from $K_{trt*}(total)$
p	Inlet pressures taken from inlet pressure gauge (on consolidometer) in "H ₂ O
e	void ratio of soil column
n	porosity of soil column

APPENDIX C

APPENDIX C

DETAILED METHODS AND MATERIALS

This appendix contains detailed descriptions of the experimental procedures used in the experiments of this study. Those procedures described herein should be used in conjunction with those previously described in the main body of the thesis.

Consolidometer Assembly

The separate pieces of the consolidometer assembly are shown in Figure 1C. Prior to any assembly, each piece of the consolidometer was cleaned and dried. In addition, the upper and lower porous stones were sonicated in 0.01 N HCl ($\text{pH} < 2$) for 12 minutes, rinsed thoroughly, and dried. Two pieces of Whatman #54 filter paper (7 cm diameter) were used for each assembly. The top filter paper was prepared by taking the cutting ring and placing it in the center of the filter paper. The inside of the cutting ring was then traced using a fine point pen. The cutting ring was then removed, and the filter paper was carefully cut along the outside edge of the traced circle. This tracing and cutting procedure produced a filter paper that would just fit inside the sample area of the cutting ring and the top ring of the consolidometer.

After cutting the top filter paper, the consolidometer base was placed on an aluminum disk so that the bottom of the valves would not elevate the base of the consolidometer (this was characterized by rocking of the consolidometer). The lower porous stone was then placed in the base of the consolidometer. Care was taken so that

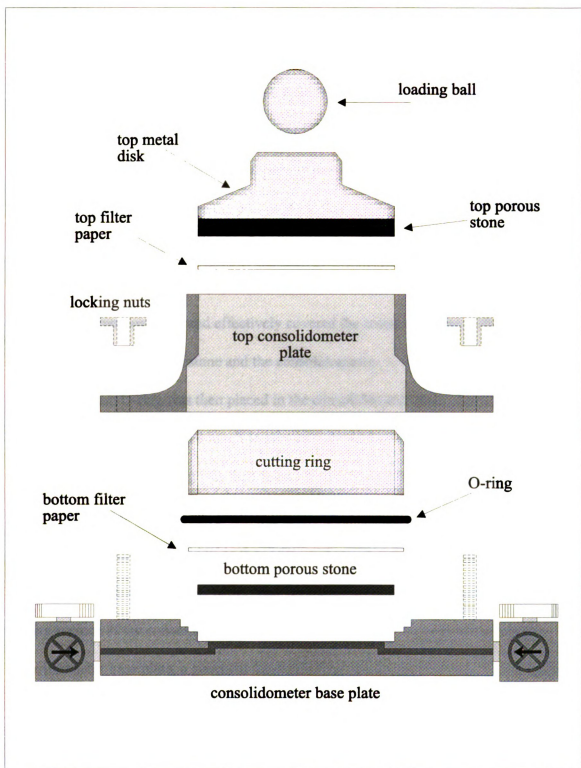


Figure 1C. Consolidometer Assembly

no particulates were present when the lower porous stone was placed in the base. To verify that no debris was lodged under the porous stone, it was spun with one hand. If no particulates were present, the porous stone spun freely, rotating several times with each spinning motion initiated by hand. If the rotation was restricted in any way, the stone was removed and the base was checked for any particulates present. The aforementioned steps were then repeated. After the porous stone was placed in the consolidometer base and was in a “free spinning” condition, the lower filter paper (the one that was not cut) was placed on top of the lower porous stone. The lower filter paper was slightly larger than the lower porous stone and effectively covered the entire diameter of the surface created by the upper porous stone and the consolidometer.

The viton O-ring was then placed in the consolidometer base. The viton O-ring had a diameter that was large enough to allow a tight seal between the O-ring and the cutting ring. The cutting ring was then seated in the consolidometer base plate by placing it in the center of the O-ring and pushing gently downward. Proper seating was achieved when the cutting ring slipped inside the O ring and rested against the filter paper resting on the metal surface of the base plate. The O-ring should have then been flush with the sealing surface of the consolidometer base. Once the cutting ring was seated in the consolidometer base plate, a generous amount of vacuum grease was placed over the O-ring. The vacuum grease was applied by placing a small amount of vacuum grease on one finger and then by running the finger around the base of the cutting ring. This should have resulted in a continuous, beveled surface of vacuum grease which completely covered the surface of the O-ring.

After application of the vacuum grease, the top consolidometer plate was placed over the threaded dowels attached to the base plate. The bottom surface of the top plate should have rested securely against the sealing surface of the base plate. The two locking screws were then placed on the threaded dowels and were tightened into place. Locking screws were tightened simultaneously to ensure proper formation of the vacuum grease seal on the sealing surface.

The consolidometer was then ready for referencing and packing of a sample (see packing section). Once a sample was packed, or if a blank conductivity experiment was to be performed, the upper porous stone was screwed into the upper metal disk. The upper filter paper was then placed on top of the sample (or placed in the middle of the consolidometer if a blank system was to be tested) followed by placement of the upper porous stone and metal disk.

Vacuum Saturation

Vacuum saturation of soil columns or blanks were achieved using a vacuum desiccator and 4 L vacuum flask, attached to a tap vacuum system. The entire vacuum system is shown in Figure 2C. Prior to any saturation procedure, the vacuum flask was filled with 1mM NaCl solution from a stock carboy. The 1mM NaCl solution was prepared by filling the carboy with distilled, deionized water to the level marked on the outside of the carboy, corresponding to 17.3 L of water. Then 1.013 g of NaCl was added to the carboy and the solution was mixed manually.

The vacuum desiccator was emptied and cleaned using tap DI water. This cleaning process was repeated at least once daily to remove any particulates and any possible build up of microbial growth. The vacuum dessicator was then filled with 1mM

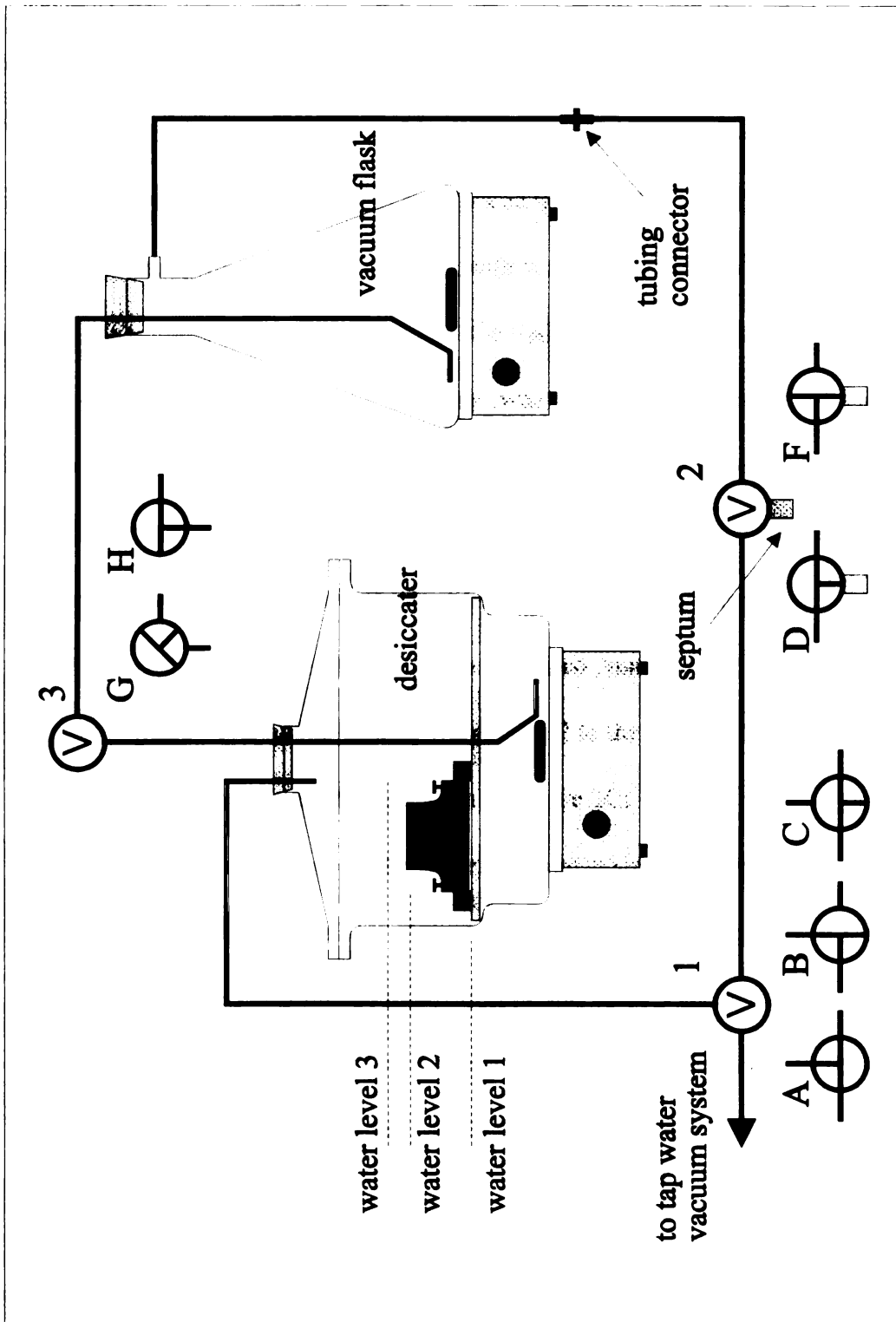


Figure 2C. Vacuum Saturation System

NaCl solution to a level just below the ceramic plate (water level 1 in Figure 2C). If the desiccater was not cleaned, excess water was poured out of the desiccater so that the remaining water filled the desiccater to water level 1.

The consolidometer containing the sample to be saturated (or blank consolidometer configuration) was then placed in the vacuum dessicater on top of the ceramic plate. Two 500 ml bottles filled with water were also placed in the desiccater to reduce the volume of water needed to fill the desiccater to levels 2 and 3 (Figure 2C) during saturation. The rim of the desiccater was coated with a thin film of vacuum grease to ensure an air tight seal. The top of the desiccater was then placed on the rim and moved laterally back and forth to ensure that a seal had formed. The appropriate tubes and stopper were then placed in the top of the desiccater. The stopper and appropriate tubes were also placed in the top of the vacuum flask, making sure that the stopper was securely in place. The tubing leading from valve 2 to the vacuum flask was then put together with a tubing connector as shown in Figure 2C.

The tube leading from the tap water vacuum system to valve 1 was then put into the vacuum connection at the base of the tap water vacuum system. Valve 1 was moved to position A, valve 2 was moved to position D, and valve 3 was moved to position G. Moving valve 3 into position G shut off any flow between the vacuum flask and the desiccater system. The building tap was then turned on, allowing a vacuum to be applied to both the vacuum flask and the desiccater. The stirrers under both the vacuum flask and the desiccater were then turned on. During the deairing process, the vacuum achieved by the system was checked with a pressure tensiometer at the septum attached to valve 2.

The vacuum achieved should have exceeded 900 mbars. Failure to reach this vacuum generally indicated a leak in the system.

The vacuum was applied to both vessels for at least one hour if a sample was to be saturated or at least 30 minutes if a blank consolidometer was to be saturated (see Blank Hydraulic Conductivity section). This time period was intended to deair the water contained in the system. At the end of the deairing period, valve 2 was turned to position F. This disconnected the vacuum from the vacuum flask. The vacuum in the vacuum flask was then released by disconnecting the tubing between valve 2 and the vacuum flask at the tubing connector. The stopper in the vacuum flask was loosened, but not removed, and the stirrer under the vacuum flask was turned off. Valve 3 was then moved to position H and water was allowed to flow from the vacuum flask to the desiccater. Flow was best (i.e. fastest) when the tubing between the vacuum flask and desiccater was hung from a nail on the wall behind the system while valve 3 was in position H. Valve 3 was left in position H until the water level in the desiccater had risen to just below the lip of the consolidometer (water level 2). Valve 3 was then moved to position G, shutting off water flow from the vacuum flask to the desiccater.

If a blank consolidometer was being saturated, the system configuration was left in the indicated configuration (valve 3 position G, valve 2 position F, valve 1 position A, tubing connector disconnected) until the saturation period was complete (30 minutes). If a sample was being saturated to be treated in an experiment, the following was performed. After the water level in the desiccater was allowed to rise to level 2 and valve 3 moved to position G, the stopper in the vacuum flask was removed and the vacuum flask was again filled with 1mM NaCl from the stock carboy. The flask was then placed

back on the stir plate and the stopper put back on the flask. The stirrer was again turned on and the tubing from valve 2 to the vacuum flask was again connected at the tubing connector. Valve 1 was then moved from position A, through position B, to position C. Valve 2 was then moved to position D. This allowed a vacuum to be applied to only the vacuum flask while preserving the vacuum in the desiccater. The vacuum was applied only to the vacuum flask until a vacuum of approximately 900 mbars had been achieved (verified by monitoring vacuum with pressure tensiometer at septum of valve 2). When the vacuum had reached this level, valve 1 was moved from position C, through position B, back to position A. The configuration was then left overnight (at least 12 hours) to allow the soil sample to completely saturate under vacuum and to allow the water in the vacuum flask to deair for use in the conductivity experiments.

At the end of the saturation period, valve 2 was moved to position F (if not in this position) and the tubing between valve 2 and the vacuum flask was disconnected (if not already disconnected), the stopper on the vacuum flask was loosened (if not loosened), the stirrer under the vacuum flask was turned off (if on), and the stirrer under the desiccater was turned off. Valve 3 was then moved to position H and the water level in the desiccater allowed to rise to water level 3, above the rim of the consolidometer. Once the water level in the desiccater rose to level 3, valve 3 was moved back to position G.

After inundating the consolidometer with water (water to level 3), the tap water was turned off. This stopped the supply of vacuum to the system. Then the tubing which connects the tap water vacuum system to valve 1 was removed from the connection to the tap water vacuum system. This released the vacuum remaining on the desiccater. Valve 2 was then moved to position D, allowing further release of the applied vacuum. Once

the vacuum had completely dissipated, the top of the desiccater was carefully removed from the desiccater and the steps for attaching the standpipe and evacuating residual air in the fittings was performed as described in later sections. The remaining water in the vacuum flask (if any) was used to supply the treatment systems and the squeeze bottles used in the conductivity experiments.

Many times during the experiments it was necessary to deair water, using the vacuum saturation system, without saturating a sample. To only deair water, the vacuum flask was first filled with 1 mM NaCl solution from the stock carboy. The stopper of the vacuum flask was then secured on top of the flask. Valve 3 was moved to position G (if not in that position already), the tubing from valve 2 to the vacuum flask was connected at the tubing connector, valve 2 was moved to position D (if not there already), and valve 1 was moved to position C. This isolated the desiccater from the vacuum so that the vacuum was applied only to the vacuum flask. The desiccater could therefore be open (without the top on). The building tap water was turned on, and the tubing from valve 1 to the tap water vacuum system was connected to the tap water vacuum system. The stirrer beneath the vacuum flask was then turned on and the water allowed to deair for at least two hours.

At the end of the deairing period, the tap water vacuum system was turned off (by turning off the water). The tubing from valve 1 to the tap water vacuum system was disconnected from the tap water vacuum system and the tubing from valve 2 to the vacuum flask was then separated at the tubing connector. This released the vacuum from the flask. The stirrer was turned off and the stopper removed from the vacuum flask. The

deaired water was then used to supply the influent reservoir in the conductivity experiments or to fill squeeze bottles.

Blank Conductivity Measurements

Blank conductivity measurements, separate from the conductivity experiments (where HDTMA treatment occurred), were performed to establish the conductivity of the system without soil and to establish a variance due to variation in the filter paper employed. Before assembling the consolidometer, prelabeled stones were sonicated in 0.1N HCL ($\text{pH} < 2$) solution for 12 minutes. Stones were then rinsed with tap water and dried manually.

The consolidometer was then assembled as shown in Figure 1C without soil. With both valves open, the consolidometer was then placed in the vacuum dessicator. The entire system was deaired by vacuum as described before for approximately 30 minutes. The water in the dessicator was then brought up to a level just below the lip of the consolidometer reservoir (water level 2 in Figure 2C). The system was then allowed to saturate for 30 minutes under vacuum. Saturation was verified by observation of water in the consolidometer reservoir.

After saturation, the blank consolidometer system was inundated with water (water level 3) and the vacuum was released (as described in Vacuum Saturation section). While the consolidometer was under water, the standpipe was attached to the consolidometer system, ensuring that no air entered the system while being attached. Any residual air left in the canal beneath the bottom porous stone was purged from the consolidometer by applying a small vacuum on the standpipe while the consolidometer remained below the water surface with both valves open. Vacuum was applied by a

rubber tube attached to the tap water vacuum system. Water was drawn into the standpipe at least four times and until no air was observed in the standpipe during application of the vacuum.

Once all of the air was purged from the consolidometer system, the valve on the inlet side of the consolidometer (the one opposite the standpipe valve) was closed. The consolidometer was then removed from the dessicator and the external parts dried manually. The reservoir of the consolidometer was partially emptied (to about half full) to allow for the seating of the middle load shaft (on load frame). The loading ball was then placed in the upper metal plate. The consolidometer was then placed in the load frame on top of an aluminum plate to elevate the valves above the stage. The consolidometer and load frame apparatus are shown in Figure 3C. Note during the blank conductivity measurements that only the consolidometer and standpipe were placed in the load frame. With the middle load shaft well above the loading ball and the low pressure regulator opened until a negative reading was observed on the pressure transducer readout, the regulator selector was moved to the low position and the load/unload valve moved to the load position. The load frame pressure was then tarred by slowing increasing the applied pressure using the low pressure regulator and observing the stage movement by relative to a reference line marked on the stage shaft beneath the stage. The low pressure regulator was then adjusted until no movement was observed, relative to the reference line on the stage shaft. Once no movement was observed, the load/unload valve was moved to the off position and the pressure output tarred by pressing the down arrow button on the pressure transducer readout. The pressure reading on the pressure transducer readout then read 0 psi. The load/unload valve was then moved to the unload

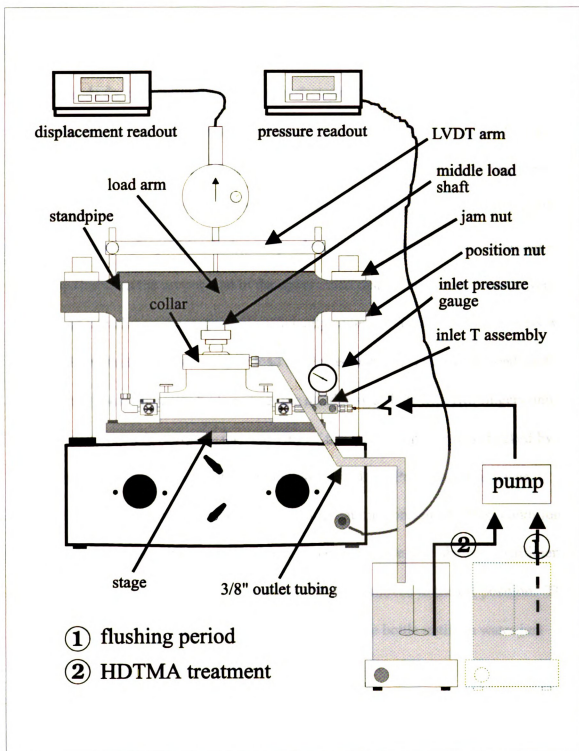


Figure 3C. Load Frame and Consolidometer Configuration

position and the stage allowed to lower to its lowermost position. For detailed instructions on the operation of the load frame and digital readouts the reader is referred to the manuals for both provided by the manufacturer.

The middle load shaft was then lowered by turning the shaft with two fingers. The consolidometer was manually adjusted to a central position while lowering the middle load shaft. The central position was verified by lifting the loading ball slightly with two fingers to the position in the receptacle of the middle load shaft and taking note of the gaps between the set position in the upper metal disk. The consolidometer was then moved laterally on the stage until sufficiently centered. This centering process was performed several times as the middle load shaft was lowered. The middle load shaft was seated on the consolidometer by lowering the middle load shaft with two fingers until a small resistance was felt. Again, the centering of the consolidometer was checked by attempting to raise the loading ball from the top metal disk. Proper centering was indicated by no movement of the ball. This configuration represented a 0 tsf condition during the blank conductivity measurements. Once the middle load shaft was sufficiently seated on the consolidometer, the load/unload valve was moved to the off position. The reservoir was filled with 1mM NaCl water from a squeeze bottle until the water just spilled from the top of the effluent reservoir.

If the extra load frame (i.e. old one) was used for the blank conductivity measurements, a slight modification of the aforementioned procedure was used. The consolidometer was placed on an aluminum metal disk on the stage of the old load frame. The aluminum metal disk was needed to ensure that the bottom of the valves did not elevate the consolidometer and create an unstable configuration. After taring the load

frame as before, the load/unload valve was moved to the unload position and the stage was allowed to move to its lowermost position. The load/unload valve was then moved to the off position. Then, a small metal ring was placed over the ball of the consolidometer. At this point, conductivities were determined as before and corresponded to the 0 tsf condition. After determination of the conductivity, the load/unload valve was moved to the load position. The low pressure regulator was then turned slowly to slightly increase the pressure on the pressure transducer readout. The stage was then allowed to raise until the metal ring which was positioned on the load ball touched the load arm and became snug. The load/unload valve was then moved to the off position. The same procedure as described in the following paragraphs was then used for the rest of the experiment.

Conductivity was then measured at the 0 tsf condition by the following procedure. Temperature measurements were then taken from both the squeeze bottle and the effluent reservoir and were recorded. These values were averaged to obtain the temperature value used for correction of conductivity to 20°C. Once the temperature readings were taken, conductivity was measured 12 times by quickly filling the standpipe with the squeeze bottle and measuring the time of drop of water between two prerecorded reference heights. Each time value was recorded individually. After twelve replicates were performed, the water in the standpipe was allowed to drop to its lowermost position (i.e. equilibrium) and this value was recorded as the datum. The procedure for measuring the conductivity conformed to the conventional falling-head permeability test with constant tail water level (ASTM D5084-90).

The load on the consolidometer was then increased to the next increment (0.25 tsf) by adjusting the load pressure regulator to the predetermined values prescribed by the manufacturer while the load/unload valve was in the off position. Once the reading of the pressure readout indicated the needed pressure, the load/unload valve was moved to the load position. This applied the 0.25 tsf load to the consolidometer system. After the load was applied to the consolidometer, the aforementioned procedure for measurement of conductivity was repeated. After measurement of conductivity at that load, the load/unload valve was moved to the off position and the pressure increased with the low pressure regulator to the next pressure corresponding to the desired effective stress. Conductivity measurements were taken at each of the following additional load conditions (0.5, 1, 2, 4, and 8 tsf). After the measurement of conductivity at the 2 tsf condition, the load/unload valve was moved to the off position as before. The regulator indicator was then moved from the low to the high position. The high pressure regulator was then used to adjust the system pressure to its desired value. While adjusting the high pressure regulator to the desired system pressure, the low pressure regulator was loosened to relieve the pressure behind the low pressure regulator valve. When the low pressure regulator moved easily, the pressure was sufficiently reduced so as not to put undue stress on the internal regulator for the course of the experiments. After hydraulic conductivity was measured at each of the effective stresses, the load/unload valve was moved to the unload position and the stage allowed to lower to its lowermost position.

Conductivity was calculated from each of the twelve time readings at each load. These values were averaged to obtain an average conductivity for at each load. A total of ten experiments were performed on each set of stones for characterization, the stones

sonicated before each experiment as before. At each load, a value of hydraulic conductivity of the stones (K_{blank}) was established by taking the average of the values of conductivity determined from the ten experiments. An uncertainty value was also established by taking twice the standard deviation of the conductivity values determined from the ten experiments. This average and uncertainty was propagated through the calculations from the conductivity experiments to establish hydraulic conductivities of the soil columns(see Calculations and Data Reduction section).

After each conductivity experiment at least one experiment with new filter paper was performed to verify the blank conductivity value assigned to the stones. This experiment was performed after determining the conductivity of the used filter papers from the experiments and before a new conductivity experiment. Stones were sonicated in acid solution, as before, prior to the experiment. Initially, one experiment was performed and the average conductivity values at each effective stress were determined as before. The values calculated were then compared to the characterization values from the ten initial experiments. If the average values from the experiment fell within the range of conductivity values determined by the initial characterization, the blank conductivity of the stones was deemed acceptable. The initial characterization values were then used for the next experiment. If the blank conductivity did not fall within the range, two additional experiments were performed with the same procedure as before. The conductivities from the three new experiments were then averaged to establish a new blank conductivity value for the stones. The higher uncertainty calculated from the three experiments and the ten initial experiments was carried as the uncertainty for the blank system.

Soil Packing / Hydraulic Conductivity Experiments

Prior to assembling the consolidometer system, the stones (prelabeled and characterized as described previously) were sonicated and dried as in the characterization experiments. The consolidometer system was then assembled, including everything except the top filter paper, top metal disk and porous stone, and loading ball. A reference puck (664 g; 6.35 cm diameter; 2.54 cm thickness) was then inserted in the consolidometer and allowed to slide along the walls of the fixed ring until seated against the bottom filter paper. The top filter paper, cut to just fit in the top ring, was then placed on top of the puck, followed by the top metal disk and porous stone assembly. The loading ball was placed in the top metal disk and the consolidometer was placed in the load frame with the load/unload valve in the unload position and the stage at its lowermost position. Prior to placing the consolidometer in the load frame, the load arm was checked to verify that it was level. The load arm was leveled using a small, two way level that could be placed on top of the load arm. Adjustments were made by loosening the jam nuts on the sides of the load arm and using the load arm position nuts (Figure 3C) to raise or lower the sides of the load arm until level. Once level, the jam nuts were tightened.

The middle load shaft was then lowered by turning the shaft with two fingers. The consolidometer was manually adjusted to a central position while lowering the middle load shaft. The central position was verified by lifting the ball slightly with two fingers to the position in the receptacle of the middle load shaft and taking note of the gaps between the set position in the upper metal disk. The consolidometer was then moved laterally on the stage until sufficiently centered. This centering process was

performed several times as the middle load shaft was lowered. The middle load shaft was seated on the consolidometer by lowering the middle load shaft with two fingers until a small resistance was felt. Again, the centering of the consolidometer was checked by attempting to raise the ball from the top metal disk. Proper centering was indicated by no movement of the ball.

Once the middle loading shaft was seated on the consolidometer, the LVDT arm was lowered until the LVDT transducer readout was approximately 0.0100-0.0200". The LVDT arm was leveled using the small level used to level the load arm and then locked into place using the locking nuts on each side of the LVDT arm. Once locked into place, the loading ball was checked to make sure that the middle load shaft was still seated. If not, the seating procedure was repeated until the loading ball did not move. Once the middle load shaft was seated, the LVDT reading was recorded as the $LVDT_{ref}$ reading. The middle load shaft was then raised until the load frame could be removed from the load frame without any contact between the middle load shaft and the loading ball.

After removing the consolidometer, the loading ball was taken off the top metal plate. The top metal plate, top porous stone, and top filter paper were then removed. The consolidometer was then inverted slightly, being careful to place a hand over the opening of the consolidometer to catch the puck, until the puck began to slide out of the consolidometer. After the puck was removed, the puck was attached to the compaction assembly if the puck was used for both referencing and packing (a new puck was used for reference while an old one was used for packing in these experiments). The compaction assembly consisted of the puck, screwed into a threaded metal dowel, and a compaction

hammer which slid along the metal dowel. The consolidometer was placed on the lab floor on top of one of the aluminum plates so the bottom of the valves did not contact the floor.

Air dried Oshtemo B soil (130 g.) was placed in a ~5 ½" aluminum pie plate. The soil was then poured in the consolidometer (the consolidometer without top filter paper, top metal plate, and top porous stone). The soil was poured into the consolidometer by slightly bending the pie plate so as to pour the soil over a smaller width and placing the bottom of the pie plate against the top rim of the top ring of the consolidometer. As the soil was poured into the consolidometer, the consolidometer was slowly turned to keep the surface of the soil in the consolidometer as level as possible. The consolidometer was turned approximately 6 to 10 complete rotations, depending on the speed with which the soil was poured. Once all of the soil was poured into the consolidometer, the pie plate was gently tapped over the consolidometer to ensure that all of the fines were removed.

The consolidometer was then tapped gently from four positions (once at each position) to further level the soil. The four positions were made by the valves on the side of the consolidometer and the consolidometer locking nuts. The compaction assembly was then carefully placed in the consolidometer until the puck (screwed onto the end of the threaded, metal dowel) rested on top of the soil. Both hands were then used to turn the entire compaction assembly four times while the puck rested on the soil. One turn consisted of a comfortable rotation achieved without removing either hand from the dowel of the compaction assembly. After four turns, the hammer of the compaction assembly (1.47 kg) was dropped onto the puck 4 times from an upper position on the rod

(7.5 cm of drop), marked by masking tape on the dowel. The compaction assembly was then carefully removed from the consolidometer so as not to disturb the compacted soil.

The top filter paper, porous stone and top metal disk, and loading ball were then placed on top of the soil in the consolidometer. Caution was used to ensure that disturbance of the upper surface of the soil did not occur during placement. The consolidometer assembly was then placed in the load frame, again with the load/unload valve in the unload position and the stage at the lowermost position. The middle load shaft was then slowly lowered onto the loading ball, centering the consolidometer as before. The middle load shaft was again seated by slowly turning the shaft with two fingers until small amounts of resistance were observed. Once the middle load shaft was seated properly, the LVDT value was recorded as the $LVDT_{pack}$.

The middle load shaft was then raised and the consolidometer removed. The loading ball was removed from the top metal disk and the consolidometer was placed in the vacuum dessicator with both valves open. The vacuum system was sealed and the water deaired under vacuum for at least one hour. After the water was deaired, the water was brought into the dessicator until the level was just below the lip of the consolidometer (water level 2, Figure 2C). The sample was then allow to saturate for at least twelve hours under vacuum. Vacuum saturation was verified after the saturation period by observation of water in the consolidometer reservoir above or around the top metal disk. At the end of saturation, water was allowed to enter the vacuum dessicator until the water level was above the rim of the consolidometer (water level 3, Figure 2C). The vacuum was then released and the top of the dessicator removed. For more details on the vacuum saturation procedure see the Vacuum Saturation section in this appendix.

While the consolidometer was still under water, the standpipe was attached to ensure that no air entered the consolidometer system. Any residual air which was left in the fittings or the canal of the consolidometer was then removed by applying a small vacuum on the standpipe while both valves were open. Water was brought into the standpipe at least four times and until no air was observed escaping from the standpipe during application of the vacuum. The valve opposite the standpipe valve was then closed and the consolidometer was removed from the dessicator.

The external parts of the dessicator system were then dried with paper towels. Small amounts of water were then removed from the effluent reservoir using paper towels. Water was removed until the level of the water was noticeably below the rim of the consolidometer. A machined collar with an outlet orifice was then placed over the rim of the consolidometer. This collar was machined to fit tightly over the consolidometer and to allow capture and recirculation of effluent solution during the conductivity experiments. Before placing the collar on the consolidometer, a small amount of vacuum grease was placed around the O-ring of the collar and on the surface of the collar that would form the contact seal with the rim of the consolidometer. The collar was placed on the consolidometer so that the outlet orifice was just above the locking nut on the right side of the consolidometer (when looking at the consolidometer from behind the standpipe). The inlet T assembly was then screwed onto the fitting attached to the inlet valve (opposite the standpipe). The T assembly consisted of an adapter fitting for connecting to the consolidometer (also an adapter fitting), a 1/4" T fitting, an adapter fitting, and a 1/16" swagelok fitting for connecting to the pump outlet tubing. A small amount of teflon tape was applied to the inlet T assembly connection

fitting before attaching it to the consolidometer. The inlet T assembly was tightened sufficiently and until the open end of the T was upright.

The loading ball was then placed on the top metal disk and the consolidometer assembly carefully placed in the load frame so as not to hit any of the added fittings. The consolidometer was oriented so that the standpipe was just in front of the left load arm support and the inlet T assembly was just behind the right load arm support (Figure 3C). As before, the load/unload valve should have been in the unload position and the stage at its lowermost position. The middle load shaft was then lowered, making slight movements of the consolidometer to center the assembly as before. The middle load shaft was then seated as before and the LVDT reading from the displacement readout recorded as the $LVDT_{sat}$ reading. Without moving the consolidometer, the middle load shaft was then raised by twisting to a displacement readout of approximately 0.4000". The load/unload valve was then moved to the off position and the regulator selector moved to the low position. The low pressure regulator was then adjusted until a negative pressure readout was observed. The inlet pressure gauge was then loosely screwed into the open end of the inlet T assembly (Figure 3C).

The load frame was then tarred by moving the load/unload valve to the load position and then slowly increasing the pressure with the low pressure regulator. As the pressure was increased the stage of the load frame moved up and the LVDT readings on the displacement readout decreased. After the stage began to move up, the pressure was adjusted with the low pressure regulator until no change in the displacement readout was observed. Caution was used to ensure that the stage did not move too far vertically in order to prevent unintentional disturbance of the sample. Once no change in the

displacement readout was observed, the load/unload valve was moved to the off position and the pressure transducer readout tarred by pressing the down arrow key on the pressure readout. The load/unload valve was then moved to the unload position and the stage allowed to move to its lowermost position. The middle load shaft was then lowered slowly by turning until the LVDT reading on the displacement readout was identical to that recorded as $LVDT_{sat}$. It was assumed that the stage position did not differ significantly in its lowermost position from that before the tarring procedure. This assumption was verified by checking the seated condition of the ball and middle load shaft on several experiments.

After lowering the middle load shaft, the unload/load valve was turned to the off position. The LVDT arm was then lowered until the LVDT readings on the displacement readout were approximately 0.2500". The LVDT arm was then leveled using the small level used before and the locking nuts of the LVDT arm were tightened. The reading on the displacement readout was then recorded as the LVDT of the sample at 0 tsf.

Before measurement of conductivity a small, flattened piece of stainless steel tubing approximately 1 ½' long was placed in the orifice of the collar that was placed on the consolidometer. A small piece of rubber tubing approximately 3" long was then placed on the end of the stainless steel tubing protruding from the collar orifice. This tubing was placed in the collar orifice to facilitate drainage of water from the effluent reservoir during the consolidation portion (and conductivity measurement) of the experiment. Without the tubing, water would rise well above the orifice opening before emptying. A build up of water behind the orifice caused difficulties in the conductivity

measurement by preventing the establishment of a stable reference datum during the falling head measurements.

Conductivity was determined at 0 tsf by falling head (ASTM D5084-90). Prior to measurement, temperatures of both the effluent reservoir and the water to be used in the test were determined with a conventional thermometer and recorded. Water (1mM NaCl), that had been deaired for at least two hours under a vacuum of approximately 900 mbars, was used as the permeant. Then, 4 falling head measurements were performed by filling the standpipe with the squeeze bottle and measuring the time for the standpipe water level to drop approximately 12 cm. Each time was recorded individually. After the four tests, the water level in the standpipe was allowed to drop to its equilibrium level. This level was recorded as the datum at this load.

After the datum was recorded for the 0 tsf load the low pressure regulator was used to increase the pressure to the pressure reading corresponding to the 0.25 tsf effective stress condition. The load/unload valve was then turned to the load position and the sample allowed to consolidate under the load. The consolidation procedure was a modified form of the conventional consolidation test (ASTM D2435-90) and was justified by Grant (thesis 1995). The samples were allowed to consolidate under each load for approximately 40 minutes, after which the load/unload valve was turned to the off position and the conductivity measured at each load using the aforementioned procedure. The pressure was then increased to the next pressure corresponding to the desired effective stress state and the load/unload valve moved to the load position, allowing the sample to consolidate under that load. The samples were consolidated

incrementally to two desired stress states (0.5 tsf and 8 tsf) using progressively larger loads as listed in the Blank Conductivity Measurements section.

Once the samples were loaded to the desired effective stress (either 0.5 or 8 tsf) and conductivities (K_o (total)) measured at that effective stress, the samples were ready for injection of solutions. An illustration of the load frame and consolidometer configuration during the flushing and treatment periods are shown in Figure 3C. Prior to the beginning the flushing period, a four liter beaker was filled with 1mM NaCl solution which was deaired for at least two hours. The inlet tubing to the pump was inserted into the solution and the pump was turned on. A diagram of the pumping system is shown in Figure 4C. Prior to this procedure, the pump had been calibrated to deliver solution at a rate of 3 mls/min. Adjustment of the delivery rate was achieved by turning the flow dial (Figure 4C). During the initial flushing of the pump(after the pump was turned on), the needle valve was adjusted until a back pressure of at least 300 psi was observed on the pump pressure gauge. The pump was then allowed to run for at least 30 minutes to ensure that any water that was not deaired was removed from the pumping system. The pump was then turned off and the pressure that built up behind the needle valve allowed to dissipate. A cover was placed on top of the inlet reservoir beaker to prevent excessive losses due to evaporation.

With the load/unload valve on the load frame still in the off position, the rubber tubing that was attached to the flattened stainless steel tubing placed in the collar orifice was separated from the flattened tubing. The stainless steel tubing was left in the orifice. A piece of 3/8" outlet stainless steel tubing was then attached using a swagelok fitting on the outlet orifice of the collar attached to the consolidometer. The outlet steel tubing

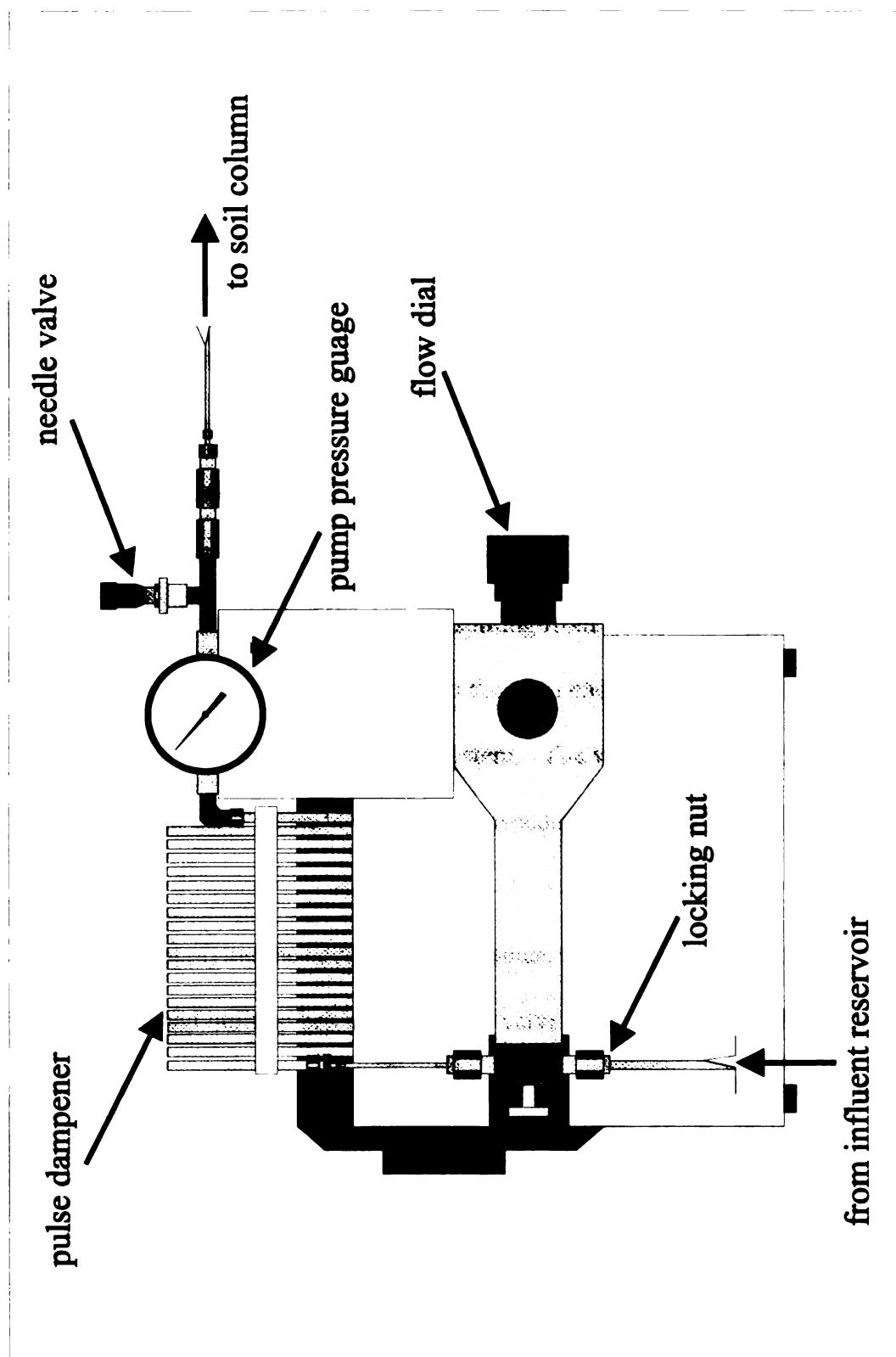


Figure 4C. Modified Pumping System for Conductivity Experiments

was then stabilized on two pieces of wood and pieces of paper and cardboard. Additional pieces of paper were inserted under the outlet tube until there was some small resistance to the insertion. The open end of the tubing was then placed in another four liter beaker positioned on a laboratory stirrer (a magnetic stirrer was placed in the beaker). A cover was then placed on the top of the outlet reservoir.

The inlet pressure gauge which had been loosely placed in the open end of the inlet T assembly was then removed. The pump outlet tube (the one which feeds solution to the consolidometer) was then attached to the inlet T assembly 1/16" swagelok fitting. The fitting was tightened until snug. The pump was then turned on and the inlet T assembly allowed to fill with water from the pumping system. Once the inlet T assembly had filled with water (verified by water spilling from the open end), a vacuum of approximately 800 mbars was applied to the open end of the T assembly using a rubber tube attached to the tap water vacuum system. The vacuum was applied for 2 minutes on the open end of the T assembly in order to evacuate any air left in the fittings of the inlet T assembly.

After applying the vacuum for 2 minutes, the pump was turned off and the pressure that had built up behind the needle valve allow to dissipate. While putting a thumb over the open end of the T assembly, the standpipe was filled with water. Before the standpipe could empty, the inlet valve (the one opposite the standpipe valve) was opened. Then water from the standpipe was allowed to flow out of the open end of the inlet T assembly by quickly moving the thumb on and off the opening. A total of four standpipes full of deaired water were emptied through the open end of the inlet T assembly by filling the standpipe and taking the thumb on and off the opening. This

procedure was intended to evacuate any air that may still have remained in the canal that was underneath the porous stone of the consolidometer.

At the completion of this step, the inlet valve was again closed and the pump turned back on. A vacuum (800mbars) was again applied to the open end of the inlet T assembly for two minutes, in an attempt to remove any air that may have not been removed by the preceding procedures. The inlet T assembly was then allowed to fill with water. After it was completely filled with water, the pump was turned off and the excess pressure that had built up was allowed to dissipate. The inlet pressure gauge was then placed in the open end of the inlet T assembly while water was above the top of the open end. Teflon tape was applied to the threads of the inlet pressure gauge in order to protect the threads and to ensure that there was a pressure tight seal. The gauge was screwed on tightly, using caution so as not to move the consolidometer system while tightening. A pressure build up was observed on the inlet pressure gauge as it was tightened. The pressure gauge was tightened as much as possible by hand.

After tightening the pressure gauge, the pump was again turned on. After observing the pressure increasing on the inlet pressure gauge (a condition that was indicative of backpressure building up behind the needle valve and therefore achieving steady flow), the inlet valve was then opened. This allowed the pump to deliver water directly to the column. The standpipe valve remained open during this procedure. A vacuum (800 mbars) was then applied to the standpipe by placing the rubber tubing over the end of the standpipe. While applying the vacuum, deaired 1mM NaCl was delivered to the effluent reservoir of the consolidometer. The vacuum caused downward flow through the column and out through the standpipe. Therefore, a continuous supply of

water was needed in the effluent reservoir to avoid desaturation of the soil column. At no time during the application of this vacuum was the water level in the effluent reservoir allowed to go below the level of the top metal disk. During application of the vacuum, a negative pressure was observed on the inlet pressure gauge. This indicated that the vacuum was applied to the entire circuit through which flow would occur in the consolidometer. The vacuum was applied for 2 minutes and was intended to evacuate any air that occurred in the entire system due to the attachment of the inlet pressure gauge. While the vacuum was applied and water was supplied to the effluent reservoir, some of the water escaped to the effluent reservoir (empty four liter beaker). If excessive air was observed in the standpipe while applying the vacuum, the seal created by the vacuum grease between the base plate of the consolidometer and the top consolidometer plate had been compromised. If further tightening of the locking screws on the consolidometer did not correct the problem, the test was abandoned.

After applying the vacuum for two minutes, the vacuum tubing was removed from the standpipe while still supplying water to the effluent reservoir. After removing the tubing, the water level in the standpipe quickly lowered. The pump was then turned off and the inlet valve closed after a small time interval. Some build up of pressure on the inlet pressure gauge was observed due to dissipation of backpressure behind the needle valve. Hydraulic conductivity was then determined as before, taking four readings of the time needed for the water level in the standpipe to drop approximately 12 cm. The average conductivity determined from the 4 readings was labeled K_{sat} (total).

Once the conductivity of the soil column was determined, the effluent reservoir was emptied and the pump was turned on again. After an increase in the inlet pressure

was observed on the inlet pressure gauge, the inlet valve was opened. The standpipe valve was then closed and 1mM NaCl solution supplied by the pump was allowed to flow directly through the column. The load/unload valve was then turned to the load position. The time at which the pump was turned on was noted as the time of the beginning of the flushing period. After a few minutes, the inlet pressure was also recorded as the inlet pressure at the beginning of the flushing period. A few minutes was needed for the inlet pressure to equilibrate with the conditions of the column.

At various time intervals during the flushing period, the effluent reservoir was sampled for turbidity and then the effluent reservoir was emptied. Readings of pump pressure, needle valve setting, inlet pressure, and displacement readout were also recorded periodically. The inlet pressures were used to calculate the hydraulic conductivity of the entire system during the flushing period ($K_{wat}(\text{total})$). The inlet reservoir was also filled at various times with 1mM NaCl solution deaired for at least 2 hours. Also during the pumping period, the buildup of excessive backpressure was relieved by slightly loosening the needle valve (see Figure 4C). Loosening of the needle valve was repeated as needed throughout the entire course of flushing and treatment. The pump pressure gauge was fairly resilient to the build up of pressures above 1000 psi. However, continued operation above this level often caused excessive fatigue of the gauge, eventually leading to necessary replacement. It should be noted that even when the pump could be kept from building up pressures above 1000 psi, some fatigue of the gauge still took place (indicated by nonzero readings when the pump was turned off). A pressure gauge with a higher range, possibly 2000 psi may remedy the fatigue problem. At no time during the flushing period was the system left without monitoring for more

that 9-10 hours. The supply of water from the inlet reservoir, even after full, was exhausted after this time interval and needed replacement.

When the period of flushing had reached 48 hours, final readings of all the aforementioned parameters were taken and the pump was turned off. The backpressure behind the needle valve was then allowed to dissipate (until the pump pressure gauge reading decreased to its lowest level and did not decrease further). The inlet valve was then closed and the standpipe valve opened. The load/unload valve was then turned to the off position. Then as before, the conductivity was measured by falling head test using 4 replicates. The average conductivity determined from the four readings was labeled K_{wat} (total).

The effluent and influent reservoir configuration was then adjusted as needed for either of the three experimental conditions used in the treatment period: no treatment (continued flushing of 1mM NaCl), low HDTMA treatment (2.16 mM HDTMA; prepared with 1350.3 mls deaired 1mM NaCl and 3.868 mls concentrated HDTMA), or high HDTMA treatment (~9mM HDTMA; prepared with 1338.1 mls deaired 1mM NaCl and 16.116 mls concentrated HDTMA). If the no treatment case was being considered, no change in the system configuration (configuration 1 in Figure 3C) was needed. The influent reservoir was filled with deaired 1mM NaCl solution (deaired for at least 2 hours). If either treatment case was being considered, the appropriate HDTMA solution was prepared in a 2000ml beaker and then was stirred gently on a laboratory stirrer. After proper mixing the effluent reservoir (4000 ml beaker) was removed from the 3/8" outlet tubing. Then, the pump inlet tube was slightly loosened to allow free lateral movement. The locking nut of the inlet tubing (Figure 4C) was slightly loosened, but not enough to

break the air tight seal that was achieved in the pumping system. Then the end of the pump inlet tube was blocked with a finger while still remaining under the surface of the water in the inlet reservoir. While still blocking the opening of the inlet tube, the influent reservoir was removed and the opening of the inlet tube placed in the HDTMA solution. The finger was then removed from the inlet tube, leaving the opening under the surface of the HDTMA solution. The HDTMA solution beaker, with the pump inlet tube still under the surface of the HDTMA solution, was then moved and placed under the 3/8" outlet tubing. The locking nut of the pump inlet tube was then tightened and a cover was placed over the solution beaker.

After the system configuration was adjusted for the appropriate experimental condition, the pump was then started again and the time of starting noted. When an increase in pressure was observed on the inlet pressure gauge, the inlet valve was opened and the standpipe valve closed. Then the load/unload valve was again turned to the load position. An initial reading of LVDT and initial inlet pressure was taken after a few minutes. The few minutes was needed to allow the inlet pressure to equilibrate with the system pressure. All readings that were taken during the flushing period were recorded periodically, except that, in the case of the HDTMA treatment cases, turbidities of the recirculated solution were not taken. Inlet pressure reading were used to calculate conductivities of the system during the treatment period, labeled K_{tr} (total). Foaming in the recirculation reservoir precluded the measurement of turbidity of these solutions. The pump pressure was again monitored as before and the needle valve loosened as needed. In the no treatment case, the influent reservoir was periodically replenished with deaired 1mM NaCl solution as was performed during the flushing period.

At the end of the 48 hour treatment period, final readings were taken and the pump was turned off, and the backpressure allowed to dissipate. The load/unload valve was then turned to the off position. The inlet valve was then closed and the standpipe valve opened. Conductivity was then determined as before on the treated soil column. The average conductivity calculated from the four falling head trials was labeled as $K_{m\cdot}$ (total).

System Dismantling

Once the conductivity was determined, the system was dismantled. The 3/8" consolidometer outlet tube was first removed from the collar on top of the consolidometer. The tube was then rinsed with tap DI water and placed on paper towels to dry. The pump outlet tubing (1/16") was then removed from the inlet T assembly. The LVDT arm was then loosened and moved up to a position that allowed free movement of the stage without the possibility of the LVDT gauge hitting the top of the middle load shaft. The load/unload switch was then moved to the unload position and the stage was allowed to move to its lowermost position. Both pressure regulators on the load frame were then loosened until a negative pressure was observed on the pressure readout when the regulator selector was in either the high or the low position (the regulator selector in the position corresponding to the regulator being loosened).

Once the stage had lowered to its lowermost position, the middle load shaft was raised by twisting until the consolidometer system could be removed from the load frame without any disturbance to the system. The consolidometer was then removed from the load frame and taken to the sink for cleaning. The flattened stainless steel tube in the outlet orifice of the collar was removed, rinsed with building DI, and placed on paper

towels to dry. Then, the inlet pressure gauge was removed from the inlet T assembly and the inside of the bourbon tube flushed with DI water using a squeeze bottle. The gauge was then gently shaken to remove any residual water which remained in the bourbon tube. The inlet T assembly was then carefully removed from the fitting on the inlet valve, making sure that the fitting on the inlet valve did not move. The inlet T assembly was then rinsed well with water and placed on paper towels to dry. After removing the inlet T assembly the inlet valve was opened and allowed to freely drain. The standpipe was then removed, rinsed, and allowed to air dry.

The loading ball was then removed from the upper metal disk, rinsed, and allowed to dry. Any excess liquid that remained in the effluent reservoir was then removed by slightly tipping the consolidometer to allow drainage over the top of the collar. The collar was then removed by prying up one end, using the handle end of a crescent wrench. The collar was subsequently rinsed with water and the vacuum grease removed using paper towels. The collar was manually dried and stored in a plastic bag for the next use. Careful handling of the collar was employed to avoid the deposition of any particulate matter that would preclude the formation of a good seal in the next experiment.

The upper metal disk and porous stone were then carefully removed and were separated. The upper metal disk was rinsed and dried. The upper porous stone was then rinsed thoroughly to remove any HDTMA solution (if any). Upon removing and cleaning the upper metal disk and porous stone, the upper filter paper that remained on the top surface of the soil column was carefully removed, rinsed gently with 1mM NaCl solution using a squirt bottle and then was placed in a 250 ml beaker of 1mM NaCl solution. Once the upper filter paper was removed, the locking screws of the

consolidometer were loosened and removed. The seal between the base plate and top plate of the consolidometer (created by the vacuum grease) was then broken by prying the top plate with a putty knife. After the seal had been broken, the top ring of the consolidometer was carefully removed. The cutting ring containing the soil column, the bottom filter paper, and the O-ring always remained connected to the top plate, so that removing the top ring also removed these pieces. Caution was always used to remove the top ring to ensure that these pieces remained connected. If the bottom porous stone remained as well, the putty knife was used to remove it before raising the top ring completely off the consolidometer base plate.

The top plate (including O-ring, bottom filter paper, cutting ring, and soil column) was then raised slightly to allow removal of the bottom filter paper. The remaining assembly was then placed on the aluminum foil storage plate constructed for sectioning of the column into sample areas for CHN analysis. The entire assemblage was placed on the storage plate in the location marked for the bottom portion of the soil column and in a manner which preserved the orientation of the soil column during the conductivity experiments (the orientation was marked on the storage surface). The bottom filter paper was then rinsed gently in the same manner as the top filter paper and was then placed in the same beaker of 1mM NaCl solution. Caution was used to place the filter papers in the same orientation as was used in the treatment experiments so as not to compromise their position when the used filter papers were later tested.

The top metal disk without the upper porous stone was then placed on top of the soil column. A slight amount of pressure was applied to the upper metal disk while raising the top consolidometer plate with both hands. This caused the cutting ring

containing the soil column, along with the O-ring, to slide free of the top ring. Upon removing the top plate, the cutting ring, O-ring, and upper metal disk remained on the storage plate. The O-ring was then removed from around the cutting ring, cleaned, and dried. Excess water around the base of the cutting ring was then removed using a paper towel. With the upper metal disk still on top of the soil column, the cutting ring was lifted slightly to allow a few fingers to be positioned under the cutting ring. Pressure was then applied to the upper metal disk while holding the cutting ring stationary with the fingers. This allowed the soil column to slide out of the cutting ring and rest on the storage plate, while remaining intact. The soil column was then covered with a paper towel moistened with 1mM NaCl, using brass rings to raise the paper towel so it was not touching the soil column. The soil column was then set aside for later sectioning.

The remaining pieces of the consolidometer (cutting ring, top ring, and base plate) were then rinsed thoroughly with building DI to remove residual HDTMA solution and then were cleaned with paper towels to remove vacuum grease. Caution was employed in cleaning the bottom portion of the consolidometer (which had valves attached and canal beneath the soil column) to make sure that all fittings were flushed well to remove HDTMA. The cleaned pieces were then placed in a storage area prior to the next experiment. The bottom porous stone was rinsed completely to remove excess HDTMA and then was placed, along with the top porous stone, in a 500 ml beaker. The stones were then covered with 0.01 N HCl solution and were sonicated for 12 minutes. The stones were then thoroughly rinsed with tap water, dried, and stored prior to further testing before the next conductivity experiment.

The load frame was then cleaned, if necessary. The pump inlet tube was removed from the recirculated HDTMA solution by loosening the locking nut of the inlet tube (Figure 4C). A portion of the recirculated solution was then placed in a 500ml glass bottle and the rest discarded. The beaker containing the recirculated solution was then cleaned and allowed to air dry. The pump inlet tube was then placed in a 4000ml beaker containing building DI water. An empty beaker was placed under the outlet tube. The pump was then turned on and the needle valve was loosened until there was no build up of back pressure observed on the pump pressure gauge. Flushing of the pump with building DI was performed for at least 12 hours, refilling the inlet reservoir and emptying the effluent reservoir as needed. This flushing step was intended to remove any residual HDTMA solution still present in the pump after the conductivity experiment.

Column Sectioning for CHN Analysis

After the cleaning of the load frame was completed and the flushing of the pump initiated, the soil column was sectioned for CHN analysis. The soil column had been placed on a storage plate covered with aluminum foil and covered with a moistened paper towel. The paper towel was removed and the brass rings moved away from the soil column. While holding a putty knife vertically along the left side of the soil column, a soil spatula was carefully inserted horizontally from the right side of the column to initiate separation of the soil column into top and bottom portions. The spatula was moved laterally back and forth to facilitate the separation. When the spatula had entered the soil column so the entire width of the spatula was in the column, the entire storage plate was rotated 90 degrees counterclockwise while the spatula was held in the same position in the soil column. The putty knife was then repositioned and held on the new

left side of the soil column. The spatula was then rotated while still within the column, using back and forth movements to further separate the column, until it was oriented in the same fashion relative to the putty knife and the entire width of the spatula was in the column. The same process was then repeated until the column was completely separated into top and bottom portions. When complete separation was achieved, the putty knife was carefully positioned within the separated column between top and bottom portions while the spatula remained in its most previous position. The top portion of the column was then raised off of the bottom portion and was positioned on the storage plate beside the bottom portion, care taken to preserve the orientation of the top portion relative to the markings on the storage plate.

The top and bottom portions now separated, the column was marked for separation as shown in Figure 5C. The inner portion was first marked by using the top of a squirt bottle and applying pressure to the top after positioning it in the center of each portion. A slight amount of pressure, just enough to make an indentation in the surface, was applied. Then, a putty knife was used to make lateral markings on each portion. Each half was partitioned into 16 regions each of which was assigned a number, shown in Figure 5C. After partitioning of the column and subsequent sampling for turbidity analysis from region 24 (Figure 5C), the storage plate was placed in a drawer and was covered with a paper towel moistened with 1mM NaCl. The paper towel was placed over brass rings so that no portion of the paper towel was touching the soil. At no time during the sectioning process was the soil touched with bare hands.

The sectioned column was allowed to dry slowly overnight. After the drying period, the storage plate was removed from the drawer. Each section of the column was

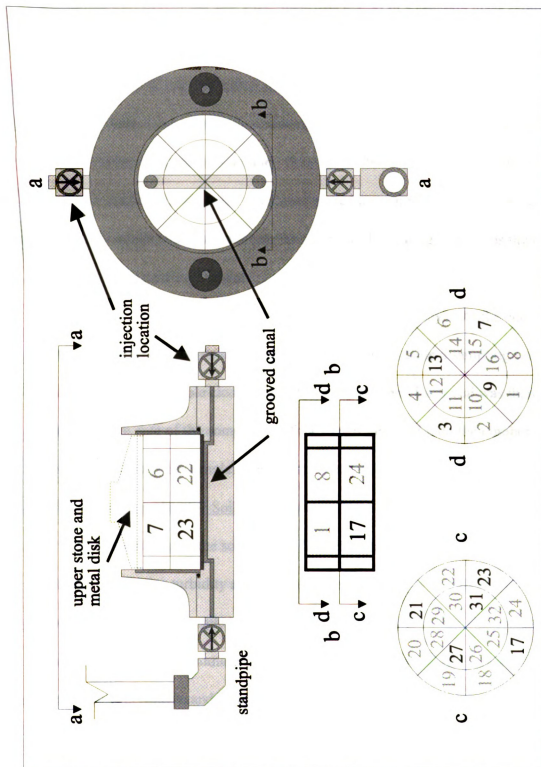


Figure 5C. CHN Analysis Numbering

then separated from the main portion of the column using a putty knife. After separation from the main portion of the soil, each piece was placed in a separate glass scintillation vial, delineated with the appropriate section number. The pieces were put into the vials using the putty knife and a sampling spatula and the pieces were not touched with bare hands at any time. The putty knife and sampling spatula were cleaned with a paper towel between the placement of each sample. Once all of the sections had been placed in the appropriate scintillation vials, the vials were placed in a safe region of the lab, away from any activities which could contaminate the samples. The storage plate was then cleaned and stored for the next experiment.

The soil samples were allowed to air dry for at least 7 days. At the end of an appropriate drying period, the soil in each vial was broken using a sampling spatula, making sure that any visible clods were sufficiently broken. Each vial was then capped and labeled with date of the completion of the experiment and with the number of its respective position. The samples were then stored until CHN analysis was performed.

Turbidity Testing of Treated Soil Columns

After sectioning of the soil column for CHN analysis, a small portion of the soil was used to determine turbidity after the treatment period. Wet soil (1.17 g) from position #24 was weighed into a sample tin. The weight of wet soil used contained approximately 1 gram of air dried soil, assuming complete saturation of the soil at the end of the conductivity experiments and an air dried water content of approximately 3%.

After weighing out 1.17 grams of wet soil, the soil was placed in a 25 ml Corex tube. Equilibrated HDTMA solution (if there was treatment 10 mls; if no treatment 10 mls of 1mM NaCl was used) from the recirculation reservoir (collected in the 500 ml

glass bottles after the treatment period) was added to the soil. The Corex tube was then sealed and agitated gently by hand for approximately 2 minutes. At the end of the agitation period, the soil suspension created was allowed to sit quiescent for 1 ½ minutes. After the settling period, a 1 ml sample of the supernate was taken from 1 cm below the liquid surface using a 1ml pipette. The sample was then diluted with 20 mls of building DI water. The turbidity of the diluted solution was then determined in the 100 range using a Hach 2400 turbidimeter. The turbidimeter was calibrated in the 100 range using the 98 NTU turbidity standard prior to the turbidity measurement. The turbidity was then determined, based on the dilution employed, and was recorded as the short term turbidity of the soil suspension for that experiment.

The Corex tube containing the rest of the soil suspension was then resealed and was placed in a rotating shaker for 4 days. At the end of the 4 day period, the Corex tube was removed from the shaker and was allowed to sit quiescent for 30 minutes. At the end of the settling period, 1 ml of supernate was taken from 1 cm below the surface. The sample was again diluted with 20 mls of building DI water and the turbidity determined as before (in 10-100 range). If the turbidity of the diluted solution was greater than 100, a 1 ml sample of the diluted solution was taken and this sample was subsequently diluted with an additional 20 mls of building DI. The turbidity of suspension was then determined as before. The turbidity of the original suspension was then calculated, based on the dilution employed, and was recorded as long term turbidity for that experiment.

Used Filter Paper Blank Conductivity Measurements

Prior to another conductivity experiment, blank conductivity measurements were made using the filter papers and the stones used in the conductivity experiment just

completed. The conductivity measurements were made to assess the loss of conductivity in the blank system due to clogging of the filter paper and the stones that may have resulted from the treatment of the soil column. The determined K_{blank} (used) value was used to calculate the K_{wat} and K_{tr} values of the flushing and treatment periods, respectively, from the K_{wat} (total) and K_{tr} (total) values determined during and at the end of each test interval.

The consolidometer was assembled as before without soil, except that the filter papers used in the treatment experiment were placed in the consolidometer. Prior to this experiment, the papers had been stored in a beaker of 1mM NaCl solution. Before the filter papers were put into the consolidometer, the papers were removed from the beaker and were dried slightly using a paper towel. The filter papers were not completely dried, but only dried enough to allow easier placement in the consolidometer system. The filter papers were placed in the consolidometer in the exact orientation as was used in the treatment experiments (i.e. sides of filter paper that were toward the soil were placed so that they were still in the same orientation).

Once the consolidometer was assembled with the used filter papers and stones from the conductivity experiment, the consolidometer was placed in the vacuum desiccator with both valves open. A vacuum was applied to the system and the water was allowed to deair for approximately 30 minutes. The water inside the desiccator was then brought up to the level just below the lip of the consolidometer (water level 2, Figure 2C) and the blank system was allowed to saturate under vacuum for at least 30 minutes. Saturation of the blank system was verified by observation of water in the consolidometer effluent reservoir above the top metal disk.

At the end of the vacuum saturation procedure, the water in the desiccater was raised above the level of the lip of the consolidometer (water level 3, Figure 2C) and the vacuum was released. While the consolidometer remained under water the standpipe was attached to the standpipe valve. As before, a slight vacuum was applied to the standpipe (with both valves open and under water) to remove any residual air left in the fittings. The inlet valve (opposite the standpipe valve) was then closed and the consolidometer was removed from the desiccater.

The consolidometer was then dried and placed in the load frame as before for blank conductivity measurements. The same procedure as was used for blank conductivity measurements was employed, except that only four measurements of the time of drop at each effective stress were taken. These four measurements were averaged to determine an average conductivity. The conductivity of the blank system using the filter papers from the experiments was calculated and labeled as mentioned before.

Calculations and Data Reduction

All conductivities determined by falling head measurements were calculated using the following equation:

$$K_{r, \bullet}(total) = \frac{2.303 \cdot a \cdot L \cdot C_t}{A \cdot t} \cdot \log \frac{(h_1 - \Delta h)}{(h_2 - \Delta h)} \quad (1C)$$

where a was the area of the standpipe (0.335 cm^2), A was the cross sectional area of the sample (31.7 cm^2), L was the total thickness through which flow occurred (including soil, if any, porous stones, and filter papers), t was the time for the drop between reference heights, C_t was a correction factor to adjust the conductivity to 20°C , h_1 was the height of the initial hydraulic head, h_2 was the height of the final hydraulic head, and Δh was the

height of the datum at equilibrium. In all cases the hydraulic conductivity calculated here represented either $K_{x*}(\text{total})$, if soil was in the consolidometer or K_{blank} , if soil was not used.

It was found experimentally that the conductivity of the stones and filter papers exerted some influence on the hydraulic conductivity of the system (because at low loads the conductivity of the soil was relatively high). Therefore, it was necessary to separate the effects of the blank system to accurately determine the hydraulic conductivity of the soil column. When conductivities of the porous stones were being measured, the hydraulic conductivity was delineated as K_{blank} . When hydraulic conductivity was measured by falling head measurements, the conductivity determined represented the conductivity of the total system, including stones and filter paper, and therefore was delineated as $K_{x*}(\text{total})$. In this labeling system, x was sat, wat, or trt, depending on the point in the experiment at which the hydraulic conductivity was determined. The notation (total) signified that the entire system was being considered. $K_{sat*}(\text{total})$ represented the hydraulic conductivity of the system after the saturation procedure had been performed (just before the beginning of the flushing period). $K_{wat*}(\text{total})$ represented the conductivity of the total system after the two day flushing period and $K_{trt*}(\text{total})$ represented the conductivity of the total system after the two day treatment period.

The hydraulic conductivities of the entire system during the flushing or treatment periods were determined from the inlet pressure taken from the inlet pressure gauge by the following equation, based on Darcy's law and assuming a constant flow rate of 3mls/min:

$$K_x(total) = \frac{(1.579 \cdot 10^{-3}) \cdot (L_{soil} + 1.6184)}{[(2.541 \cdot p) - (L_{soil} + 2.5184)]} \quad (2C)$$

where L_{soil} was the length of the soil (cm.) and p was the recorded inlet pressure ("H₂O).

The other terms in the equation were determined by reduction of Darcy's law to calculation of hydraulic conductivity. The hydraulic conductivities calculated by this method also represent the hydraulic conductivity of the entire system and were therefore with the same subscripts mentioned earlier, depending on which experimental period from which the pressures were taken. Note that the asterisks were not included in the subscripts of the conductivities calculated from inlet pressures.

As was mentioned previously, it was necessary to separate the effects of the porous stones and the filter papers to more accurately determine the hydraulic conductivity of the soil. Using the conductivity of the blank consolidometer system (K_{blank}) and the conductivity of the total consolidometer system including soil ($K_{x*}(total)$ or $K_x(total)$), the hydraulic conductivity of the soil column was calculated using the following equation, derived from a layered soil system:

$$K_{x*} \text{ or } K_x = \frac{L_{soil} \cdot [K_{x*}(total) \text{ or } K_x(total)] \cdot K_{blank}}{[(L_{total} \cdot K_{blank}) - ([K_{x*}(total) \text{ or } K_x(total)] \cdot L_{blank})]} \quad (3C)$$

where K_{x*} or K_x was the conductivity of the soil column at various periods during the experiment (cm/s), L_{soil} was the length of the soil column at the time of measurement of hydraulic conductivity (cm), $K_{x*}(total)$ or $K_x(total)$ was the hydraulic conductivity of the entire system (cm/s), K_{blank} was the hydraulic conductivity of the blank at the time of the conductivity measurement (cm/s), L_{total} was the length of the entire system at the

time of the measurement (cm), and L_{blank} was the length of the stones and filter papers (cm). This equation was used to calculate the hydraulic conductivity of the soil column at both the end points of the treatment periods (based on total hydraulic conductivity measured by falling head) and during the treatment periods (when total conductivity was calculated from inlet pressure by equation 2C).

Some clarification of the specific values of hydraulic conductivity used to calculate certain soil hydraulic conductivities is needed. For all values of K_x^* or K_x , the corresponding K_x^* (total) or K_x (total) value was used. The K_{blank} value used depended on the point of measurement. The values of each conductivity parameter used to calculate the corresponding soil hydraulic conductivity at the endpoints of treatment (i.e. based on falling head measurements) are summarized in Table 1C.

The calculations of soil hydraulic conductivity during the flushing and treatment periods was less straightforward. As was mentioned earlier, total hydraulic conductivities were calculated from a derived empirical formula, based on values of inlet pressure recorded during the flushing and treatment periods. Although close, the calculated total conductivity at the beginning and end of the flushing and treatment periods did not correspond to the value of conductivity derived from falling head measurements (i.e. at beginning and end of each period). It was therefore necessary to use an add factor to adjust the pressure so the total hydraulic conductivity agreed with the value calculated from the falling head measurements. A different add factor was needed at the beginning and the end of each period and was determined by trial and error at each point. Therefore, it was necessary to interpolate the value of the add factor, based on the change in total conductivity at the specific time in the flushing or treatment period compared to

Table 1C. Values of Hydraulic Conductivity Used to Calculate Soil Conductivities from Falling Head Measurements

Description	soil K calculated	total K used	K_{blank} used
soil hydraulic conductivity after saturation of the consolidometer system (just before beginning of flushing period)	K_{sat}	K_{sat}^* (total)	interpolated value between K_{blank} and K_{blank} (used) based on change in total K (between K_o (total) and K_{sat} (total))
soil hydraulic conductivity after 2 day flushing period	K_{wat}	K_{wat}^* (total)	interpolated value between K_{blank} and K_{blank} (used) based on change in total K (between K_o (total) and K_{wat} (total))
soil hydraulic conductivity after 2 day treatment period	K_{rrt}	K_{rrt}^* (total)	K_{blank} (used)

the total change in total conductivity observed during that period. It should be noted that the value of K_{blank} used at each time of conductivity determination during the flushing and treatment periods was calculated by interpolation. As was the case in the conductivities determined by falling head, the K_{blank} used at each specific point was determined by interpolating between K_{blank} and the K_{blank} determined on the used filter papers, based on the change in total hydraulic conductivity at that point compared to the total change in total hydraulic conductivity observed throughout the experiment. The values of each parameter used for calculation of soil hydraulic conductivity during the flushing and treatment periods are summarized in Table 2C.

Lengths of the system and soil were based on LVDT readings taken at various times during the experiment. The length of the porous stones and filter papers (i.e. L_{blank}) was assumed to remain constant throughout the experiments. L_{blank} was determined to be 1.6184 cm, based on measurement of the stones with calipers and the manufacturer standards for the filter paper. The length of the soil prior to any consolidation was based on the reference LVDT reading ($LVDT_{ref}$) taken with the machined brass puck in the consolidometer assembly and the LVDT readings taken after packing ($LVDT_{pack}$) or after sample saturation ($LVDT_{sat}$). The length of the soil column and the length of the entire system(cm.) prior to experiments was calculated from the following equations:

$$L_{soil}(pack, sat) = 2.54 \cdot \left[1 + \left(LVDT_{pack, sat} - LVDT_{ref} \right) \right] \quad (4C)$$

$$L_{total}(pack, sat) = L_{soil}(pack, sat) + 1.6184 \quad (5C)$$

Table 2C. Values of Hydraulic Conductivity Used to Calculate Soil Conductivities from Inlet Pressure Measurements

Description	soil K calculated	added factor used	total K used	K_{blank} used
soil hydraulic conductivity during the 2 day flushing period	K_{wat}	interpolated value between added factors determined for the endpoints of flushing period based on change in K (total) compared to total change in K(total) during flushing period	$K_{wat}(\text{total})$ calculated from recorded inlet pressure (plus interpolated added factor)	interpolated value between K_{blank} and $K_{blank}(\text{used})$ based on change in K(total) compared to change in K(total) over entire experiment
soil hydraulic conductivity during the 2 day treatment period	K_{trt}	interpolated value between added factors determined for the endpoints of treatment period based on change in K (total) compared to total change in K(total) during treatment period	$K_{trt}(\text{total})$ calculated from recorded inlet pressure (plus interpolated added factor)	interpolated value between K_{blank} and $K_{blank}(\text{used})$ based on change in K(total) compared to change in K(total) over entire experiment

Based on the method used to determine the lengths of the system, the length of the soil column (and entire system) at 0 tsf was equal to the corresponding length after saturation, determined from equations 4C and 5C. Therefore, the length of the soil or entire system was determined from the LVDT reading at the point the length was desired compared to the LVDT at 0 tsf (recall that the LVDT arm was moved after recording $LVDT_{sat}$ and was therefore different from that reading). The following equations were used to calculate the length of the soil and lengths of the entire system (cm) at any time in the experiments:

$$L_{soil}(0tsf) = L_{soil}(sat) \quad (6C)$$

$$L_{soil}(load, sat, wat, trt) = L_{soil}(0tsf) - \left[2.54 \cdot (LVDT_{0tsf} - LVDT_{load, sat, wat, trt}) \right] \quad (7C)$$

$$L_{total}(load, sat, wat, trt) = L_{soil}(load, sat, wat, trt) + 1.6184 \quad (8C)$$

Porosity of the soil samples was calculated at each point during consolidation and during the flushing and treatment periods. The porosity was calculated based on the length of the soil column using the following equation:

$$n = \frac{V_v}{V_t} = \frac{(A \cdot L_{soil}) - \frac{M_s}{G_s}}{(A \cdot L_{soil})} \quad (9C)$$

where n was the porosity (no units), V_v was the volume of the pore space (cm^3), V_t was the total volume of the sample (cm^3), A was the area of the sample (31.7 cm^2), L_{soil} was the length of the soil column (cm), M_s was the mass of solids used in the experiment (130.00 g), and G_s was the specific gravity of the soil solids (here assumed to be 2.65).

Uncertainty was propagated through all calculations based on statistical analysis. This propagation, while straightforward in its application, involved relatively complex equations. Therefore, the exact equations used for each is not mentioned here. The

reader is referred to calculation sheets included in records kept during the experiments and to the spreadsheets used in the calculations.

APPENDIX D

APPENDIX D

ENGINEERING APPLICATION

The creation of sorption zones by *in-situ* injection of HDTMA in soils with dispersed clays appears hydraulically feasible. Although changes in the dimensions of the sorptive zone may be appropriate to account for changes in hydraulic conductivity, the data presented indicate that the sorptive zones will function favorably in groundwater flow situations. Furthermore, no substantial changes in the porosity of the soil columns was observed during the experiments, suggesting that no significant changes in soil volume will occur due to treatment.

In field situations, the installation of wells and injection of HDTMA treatment solution would obviously disturb the soil matrix for several reasons. First, it is likely that an increased rate of flow would be needed for the injection to take place. Therefore some reorientation of the soil matrix due to high hydraulic gradients would be expected. Second, if the injected solution had different chemical properties relative to the indigenous pore solution, some change in the character of the clays may occur due to the reestablishment of equilibrium conditions between the soil exposed to the flow and the injected solution. Third and finally, the presence of HDTMA in the injected solution will likely impart changes in the degree of clay dispersion, depending on the indigenous condition of the clays before treatment and on other factors influencing the mechanism of HDTMA sorption.

Based on the experimental results presented and based on the preceding discussion, several general recommendations can be made as to the method of *in-situ* soil modification using HDTMA surfactant. First, every effort should be made to mimic the chemistry of the indigenous soil water in the treatment solution. It is obvious from the experimental results that changing the solution chemistry does have an effect on the hydraulic conductivity of soils. Second, treatment of soils to HDTMA levels up to the CEC of the soil, whether through a recirculation or a continuous injection scenario should better preserve the hydraulic conductivity of the soil and result in a stable HDTMA clay complex. The treatment of soils to an HDTMA concentration higher than the CEC may result in larger decreases in conductivity and these decreases may become even more pronounced as the clay fraction of the soil becomes larger. In addition to higher decreases in hydraulic conductivity, hydrophobically bonded HDTMA that would present at high treatment levels may be detrimental to the feasibility of sorptive zones. It has been found that significant desorption of hydrophobically bonded HDTMA occurs when added to a soil at levels above the CEC (Zhang *et al.* 1993; Xu and Boyd 1995a) and that HDTMA in the aqueous phase is toxic to pollutant degrading bacteria (Nye *et al.* 1994). Therefore, desorption of hydrophobically bonded HDTMA may interfere with retardation of contaminants (if contaminants which partition into the HDTMA clays are released as HDTMA is desorbed) and may be harmful to biodegradation techniques coupled with the sorptive zone concept. In addition, dispersion of soil clays caused by the hydrophobic bonding of HDTMA may result in significant migration of clays. Sorbed contaminants on these clays may be transported by the flow, a process often termed facilitated transport (Govindaraju *et al* 1995), thus interfering with the retardation of the contaminants.

However, treatment of soils with higher HDTMA concentrations may overcome delivery limitations exerted by field heterogeneities, as evidenced by the differences in HDTMA distribution between high and low treatment shown in Table 2. It may be feasible, then, to inject higher concentrations of HDTMA followed by an extended flushing period to redistribute hydrophobically bonded HDTMA to downgradient ion exchange sites. This would result in a more stable HDTMA clay sorptive zone. Further research is needed to evaluate the hydraulic consequences of this scenario.

LIST OF REFERENCES

LIST OF REFERENCES

- Allred, B. and G.O. Brown. 1994. "Surfactant-Induced Reductions in Soil Hydraulic Conductivity." Groundwater Management and Remediation Spring: 174-184.
- Alther, G.R., J.C. Evans, and S.E. Pancoski. 1990. "No Feet of Clay." Civil Engineering August: 60-61.
- Blowes, D.W., C.J. Ptacek, J.A. Cherry, R.W. Gillham, and W.D. Robertson. 1995. "Passive Remediation of Groundwater Using *In Situ* Treatment Curtains." In *Geoenvironment 2000*. Proceedings of the Specialty Conference on Geotechnical Practice. B.A. Yalcin and D.E. Daniel (Eds.), ASCE, New York, NY, vol. 2: 1588-1607.
- Bowders, J.J. 1985. "The Influence of Various Concentrations of Organic Liquids on the Hydraulic Conductivity of Compacted Clay." Dissertation GT85-2, Civil Engineering Dept., U. Texas, Austin, TX.
- Bowders, J.J. and D.E. Daniel. 1987. "Hydraulic Conductivity of Compacted Clay to Dilute Organic Chemicals." Journal of Geotechnical Engineering 113(12): 1432-1448.
- Boyd, S.A., J.F. Lee, and M. M. Mortland. 1988. "Attenuating Organic Contaminant Mobility by Soil Modification." Nature 33: 345-347.
- Boyd, S.A., W.F. Jaynes, and B.S. Ross. 1991. "Immobilization of Organic Contaminants by Organo-clays: Application to Soil Restoration and Hazardous Waste Containment." In *Organic Substances and Sediments in Water*. R.A. Baker (Ed.), CRC Press, Boca Raton, FL, Vol. 1: 181-200.
- Brown, K.W. and J.C. Thomas. 1987. "A Mechanism by which Organic Liquids Increase the Hydraulic Conductivity of Compacted Clay Materials." Soil Science Society of America Journal 51:1451-1459.
- Burris, D.R. and C.P. Antworth. 1990. "Potential for Subsurface In-Situ Sorbent Systems." Groundwater Management. 4: 527-538.

Burris, D.R. and C.P. Antworth. 1992. "In situ Modification of an Aquifer Material by a Cationic Surfactant to Enhance Retardation of Organic Contaminants." Journal of Contaminant Hydrology 10: 325-327.

Collins, K. and A. McGown. 1974. "The Form and Function of Microfabric Features in a Variety of Natural Soils." Geotechnique 24(2): 223-254.

Crocher, F. H., W.F. Guerin, and S. A. Boyd. 1995. "Bioavailability of Naphthalene Sorbed to Cationic Surfactant-Modified Clay." Environmental Science and Technology 29: 2953-2958.

Daniel, D.E. 1994. "State-of-the-Art: Laboratory Hydraulic Conductivity Tests for Saturated Soils." In *Hydraulic Conductivity and Waste Contaminant Transport in Soil*. ASTM STP 1142 D.E. Daniel and S.J. Trautwein (Eds.): 30-78.

Eykholt, G.R. and T.M. Sivavec. 1995. "Contaminant Transport Issues for Reactive Permeable Barriers." In *Geoenvironment 2000*. Proceedings of the Specialty Conference on Geotechnical Practice. B.A. Yalcin and D.E. Daniel (Eds.), ASCE, New York, NY, vol. 2: 1608-1621.

Evans, J.C., S.E. Pancoski, and G. Alther. 1989. "Organic Waste Treatment with Organically Modified Clays." Res. Dev. [Rep.] EPA/600/9-89/072, International Conference on New Frontiers in Hazardous Waste Management, 3rd: 48-58.

Evans, J.C. and S.E. Pancoski. 1989. "Organically Modified Clays." Transportation Research Record 1219: 160-168.

Fernandez, F. and R.M. Quigley. 1991. "Controlling the Destructive Effects of Clay-Organic Liquid Interactions by Application of Effective Stresses." Canadian Geotechnical Journal 28: 388-398.

Goldenberg, L.C., I. Hutcheon, N. Wardlaw, and A.J. Melloul. 1993. "Rearrangement of Fine Particles in Porous Media Causing Reduction of Permeability and Formation of Preferred Pathways of Flow: Experimental Findings and a Conceptual Model." Transport in Porous Media 13: 221-237.

Govindaraju, R.S., L.N. Reddi, and S.K. Bhargava. 1995. "Characterization of Preferential Flow Paths in Compacted Sand-Clay Mixtures." Journal of Geotechnical Engineering 121(9): 652-659.

Hatfield, K., D. Burris, T.B. Stauffer, and J. Ziegler. 1992. "Theory and Experiments on Subsurface Contaminant Sorption Systems." Journal of Environmental Engineering 118(3): 322-337.

Holtz, R.D. and W.D. Kovacs. 1981. *An Introduction to Geotechnical Engineering*. Prentice-Hall, Inc., Englewood Cliffs, NJ.

Jaynes, W.F. and S.A. Boyd. 1991. "Hydrophobicity of Siloxane Surfaces in Smectites as Revealed by Aromatic Hydrocarbon Adsorption from Water." Clays and Clay Minerals 39(4): 428-436.

Kenney, T.C., W.A. van Veen, M.A. Swallow, and M.A. Sungaila. 1992. "Hydraulic Conductivity of Compacted Bentonite-Sand Mixtures." Canadian Geotechnical Journal 29: 364-374.

Lambe, W.T. 1958a. "The Structure of Compacted Clay." Journal of the Soil Mechanics and Foundations Division 84(SM2): 1654-1 - 1654-34.

Lambe, W.T. 1958b. "The Engineering Behavior of Compacted Clay." Journal of the Soil Mechanics and Foundations Division 84(SM2): 1655-1 - 1655-35.

Lee, J.F., J.R. Crumb, and S.A. Boyd. 1989. "Enhanced Retention of Organic Contaminants by Soils Exchanged with Organic Cations." Environmental Science and Technology 23: 1365-1372.

Levy, G.J., I. Shainberg, N. Alperovitch, and A.J. van der Merwe. 1991. "Effect of Na-Hexametaphosphate on the Hydraulic Conductivity of Kaolinite-Sand Mixtures." Clays and Clay Minerals 39(2):131-136.

Mitchell, J.K. 1976. *Fundamentals of Soil Behavior*. 1st Edition, John Wiley & Sons, Inc., New York.

Mitchell, J.K. and F. T. Madsen. 1987. "Chemical Effects on Clay Hydraulic Conductivity." In *Geotechnical Practice for Waste Disposal*. ASCE STP 13: 87-116.

Nye, J. V., W.F. Guerin, and S.A. Boyd. 1994. "Heterotrophic Activity and Microorganisms in Soils Treated with Quaternary Ammonium Cations." Environmental Science and Technology 28: 941-944.

Olsen, R.E. and D.E. Daniel. 1981. "Measurement of the Hydraulic Conductivity of Fine-Grained Soils." In *Permeability and Groundwater Contaminant Transport*. ASTM STP 746: 18-64.

Quigley, R.M. and F. Fernandez. 1989. "Clay/Organic Interactions and Their Effect on the Hydraulic Conductivity of Barrier Clays." In *Contaminant Transport in Groundwater* Kobus and Kinzelbach (Eds.), Balkema, Rotterdam: 639-691.

Rao, S.N. and P.K. Mathew. 1995. "Effects of Exchangeable Cations on Hydraulic Conductivity of a Marine Clay." Clays and Clay Minerals 43(4):433-437.

Roy, S.B. and D. A. Dzombak. 1995. "Colloid Release and Transport Processes in Natural and Model Porous Media." ACS Preprints of Papers Presented at the 209th ACS National Meeting 35 (1): 501-504.

Sai, J.O. and D.C. Anderson. 1992. "Barrier Wall Materials for Containment of Dense Nonaqueous Phase Liquids (DNAPL)." Hazardous Waste and Hazardous Materials 9(4): 581-585.

Shackelford, C.D. 1994. "Waste-Soil Interactions That Alter Hydraulic Conductivity." In *Hydraulic Conductivity and Waste Contaminant Transport in Soil*. ASTM STP 1142, D.E. Daniel and S.J. Trautwein, Eds., American Society for Testing and Materials, Philadelphia, PA.: 111-168.

Shelley, T.L. and D.E. Daniel. 1993. "Effect of Gravel on Hydraulic Conductivity of Compacted Soil Liners." Journal of Geotechnical Engineering 199(1): 54-68.

Sheng, G., S. Xu, and S.A. Boyd. 1996a. "Mechanisms Controlling Sorption of Neutral Organic Contaminants by Surfactant Derived and Natural Organic Matter." Environmental Science and Technology 30: 1553-1557.

Sheng, G., S. Xu, and S.A. Boyd. 1996b. "Cosorption of Organic Contaminants from Water by Hexadecyltrimethylammonium-Exchanged Clays. Water Research 30: 1483-1489.

Smith, J.A. and P.R. Jaffe'. 1994. "Benzene Transport Through Landfill Liners Containing Organophilic Bentonite." Journal of Environmental Engineering 120(6): 1559-1577.

van Olphen, H. 1977. *An Introduction to Clay Colloid Chemistry*. 2nd Edition, John Wiley & Sons, New York, NY.

Wallace, R.B., J.M. Grant, T.C. Voice, G.R. Rakhshandehroo, S. Xu, and S.A. Boyd. 1995. "Hydraulic Conductivity of Organomodified Soil." In *Innovative Technologies for Site Remediation and Hazardous Waste Management*. Proceedings of ASCE 1995 National Conference on Environmental Engineering. R.D. Vidic and F.G. Pohland (Eds.), ASCE, New York, NY: 92-100.

Xu, Shihe and S.A. Boyd. 1994. "Cation Exchange Chemistry of Hexadecyltrimethylammonium in Vermiculite Subsoils." Soil Science Society of America Journal 58: 1382.

Xu, Shihe and S.A. Boyd. 1995a. "Cationic Surfactant Sorption to a Vermiculite Subsoil via Hydrophobic Bonding." Environmental Science and Technology 29(2): 312-320.

Xu, Shihe and S.A. Boyd. 1995b. "Cationic Surfactant Adsorption by Swelling and Nonswelling Layer Silicates." Langmuir 11: 2508-2514.

Xu, Shihe and S.A. Boyd. 1995c. "An Alternative Model for Cationic Surfactant Adsorption by Layer Silicates." Environmental Science and Technology 29: 3022-3028.

Yang, N. and S.L. Barbour. 1992. "The Impact of Soil Structure and Confining Stress on the Hydraulic Conductivity of Clays in Brine Environments." Canadian Geotechnical Journal 29: 730-739.

Yong, R.N. and B.P. Warkentin. 1975. *Soil Properties and Behaviour*. Elsevier Scientific Publishing Co., Amsterdam.

Zhang, Z.Z., D.L. Sparks, and N.C. Scrivner. 1993. "Sorption and Desorption of Quaternary Amine Cations on Clays." Environmental Science and Technology 27(8): 1625-1631.

MICHIGAN STATE UNIV. LIBRARIES



31293015818986